NASA-TM-112829

Constraints on Martian differentiation processes from Rb-Sr and Sm-Nd isotopic analyses of the basaltic shergottite QUE 94201

Lars E. Borg[1], Larry E. Nyquist[1], Larry A. Taylor[2], Herny Wiesmann[3], and Chi -Y. Shih[3]

1. SN4/NASA Johnson Space Center, Houston TX 77058
2. Department of Geological Sciences, University of Tennessee, Knoxville TN 3799
3. Mail Code C23, Lockheed Martin, 2400 NASA Road 1, Houston TX 77258

ABSTRACT

Isotopic analyses of mineral, leachate, and whole rock fractions from the Martian shergottite meteorite QUE 94201 yield Rb-Sr and Sm-Nd crystallization ages of 327±12 and 327±19 Ma, respectively. These ages are concordant, although the isochrons are defined by different fractions within the meteorite. Comparison of isotope dilution Sm and Nd data for the various QUE 94201 fractions with in situ ion microprobe data for QUE 94201 minerals from the literature demonstrate the presence of a leachable crustal component in the meteorite. This component is likely to have been added to QUE 94201 by secondary alteration processes on Mars, and can affect the isochrons by selectively altering the isotopic systematics of the leachates and some of the mineral fractions. Initial $^{87}Sr/^{86}Sr$ of 0.701298±12, ε_{Nd}^{143} of 47.6±1.7, and whole rock ε_{Nd}^{142} of 0.92±0.11 indicate that QUE 94201 was derived from a source that was strongly depleted in $^{87}Rb/^{86}Sr$ and enriched in $^{147}Sm/^{144}Nd$ early in its history. Partial melting models demonstrate that the Sm-Nd isotopic compositions of QUE 94201 can be produced from a single chondritic source by no fewer than five episodes of melting; two occurring at 4.525 Ga and three at 327 Ma, and that the source was not significantly melted between 4.525 Ga and 327 Ma. Rb-Sr-based partial melting models are unable to reproduce the composition of QUE 94201 using the same model parameters employed in the Sm-Nd-based models, implying a decoupling of Rb-Sr and Sm-Nd isotopic systems. The initial decoupling of the two isotopic systems can be attributed to multiple melting events which are able to more efficiently fractionate Rb from Sr (into crustal and mantle reservoirs) compared to Sm from Nd. The fact that all Martian meteorites analyzed so far define a Rb-Sr whole rock isochron age of 4.5 Ga suggests that virtually all Rb was partitioned into the crust at that time. Thus, the Martian mantle is not expected to evolve past $^{87}Sr/^{86}Sr$ of 0.700, and could not have been significantly enriched in Rb by crustal recycling processes. All Martian meteorites have initial $^{87}Sr/^{86}Sr$ values that are higher than ~0.700, and are likely to be produced by mixing between crustal and mantle reservoirs. The absence of crustal recycling processes on Mars may preserve the geochemical evidence for early differentiation and the decoupling of the Rb-Sr and Sm-Nd isotopic systems, underscoring one of the fundamental differences between geologic processes on Mars and the Earth.

INTRODUCTION

A recently identified SNC (Shergotty-Nakhla-Chassigny) meteorite is the basaltic shergottite QUE 94201. Despite the fact that the meteorites belonging to this group include basalts and lherzolites (shergottites), pyroxenites (nakhlites and ALH 84001), and a dunite (Chassigny), they all share geochemical and isotopic affinities that are consistent with a Martian origin (e.g., McSween, 1994). Although QUE 94201 has abundances of major elements that are roughly similar to those of other shergottites, particularly EETA 79001 lithology B, it demonstrates the most extreme geochemical fractionations of any Martian meteorite studied thus far (Mittlefehldt and Lindstrom, 1996). High field strength elements (HFSE), such as P, Hf, and Ti, as well as middle-rare earth elements (MREE) to heavy-REE (HREE), are significantly higher in QUE 94201 than in the other shergottites, whereas abundances of the most incompatible elements, such as Rb, K, Ta, and light-REE (LREE), are as low or lower than the most depleted shergottites (Fig. 1). This is consistent with the fact that QUE 94201 has the most strongly LREE-depleted chondrite-normalized REE pattern of any Martian meteorite. These observations have led to the suggestions that 1) QUE 94201 was derived from a source that was strongly depleted through melting events, and 2) the melt was not significantly modified by the addition of the LREE-enriched crustal component that is present in the other shergottites (Gleason et al. 1996; Kring et al. 1996). Thus, QUE 94201 potentially offers strong constraints on the mineralogy and composition of SNC mantle sources, the extent and timing of melting events on Mars, and the petrogenetic relationships among the individual meteorites.

We have completed Rb-Sr and Sm-Nd isotopic analyses of minerals, whole rocks, and leachates from QUE 94201. This sample is older than the other shergottites, and has isotopic compositions that indicate it was derived from a source that was strongly depleted in incompatible elements early in its history. We also present time-integrated melting models that demonstrate that QUE 94201 can be derived from a primitive (chondritic) mantle that has undergone repeated small-volume partial melting events. The initial melts could represent early-formed Martian crust, and would have very low present-day $^{147}Sm/^{144}Nd$, ε_{Nd}^{143} values, and high $^{87}Rb/^{86}Sr$ and $^{87}Sr/^{86}Sr$

values. Conversely, the mantle source of QUE 94201 must have very high present-day $^{147}Sm/^{144}Nd$ and ε_{Nd}^{143}, as well as low $^{87}Rb/^{86}Sr$ and $^{87}Sr/^{86}Sr$ values. The REE and isotopic systematics of the other shergottites are consistent with melts derived from a variably depleted (QUE 94201-like) source that have assimilated small amounts of early-formed highly fractionated crust.

PETROGRAPHY

We present a brief petrographic description to familiarize the reader with the mineral fractions that are used to define Rb-Sr and Sm-Nd isochrons discussed later. Petrographic and electron microprobe analysis of QUE 94201 by Harvey et al. (1996), Kring et al. (1996), McKay et al. (1996), McSween and Eisenhour (1996), McSween et al., (1996), and Mikouchi et al. (1996) demonstrate that it is composed of about 35-44% clinopyroxene, 32-46% maskelynite (diaplectic glass formed from shocked plagioclase), 18-30% impact melt, 4-5% whitlockite, 2-3% opaque oxides (ilmenite, ulvöspinel, pyrrhotite, Fe-Ti oxide), and 4% mesostasis (fayalite, feldspar, whitlockite, silica, pyroxferroite, chlorapatite, rutile, and possible baddeleyite). Fe, K, and Ca sulfates have also been observed in QUE 94201 and have been interpreted as products of low temperature water-based alteration of the meteorite on Mars or in Antarctica (Harvey et al., 1996; Wentworth and Gooding, 1996). Maskelynite ranges from An_{68} to An_{52}. Pigeonite and augite coexist in QUE 94201 and are strongly zoned to Fe-rich rims. Pyroxene cores are typically Mg-rich pigeonite (with compositions near $Fs_{30}Wo_{15}$) mantled by Mg-rich augite (~$Fs_{20}Wo_{35}$), and are rimmed by Fe-rich pigeonite (up to Fs_{85}) that is zoned to pyroxferroite. Zoning patterns in these pyroxenes are similar to those in several Apollo 15 quartz-normative basalts, and like the zoning patterns in the Apollo 15 pyroxenes, have been interpreted to reflect crystallization in a closed system (Kring et al., 1996; McSween and Eisenhour, 1996; McSween et al., 1996). Thus, unlike the other shergottites, QUE 94201 does not contain cumulus minerals, and is therefore likely to have a composition that more closely reflects a Martian magma.

GEOCHEMICAL CONSTRAINTS ON SNC PETROGENESIS

Major- and trace-element chemistry, and isotopic systematics of the SNC meteorites place strong constraints on the mineralogy and composition of their sources, the extent and timing of melting events, and petrogenetic relationships among the individual meteorites. There is a strong decoupling of REE abundances and Nd isotopic systematics in the SNC meteorites. Nakhlites and Chassigny, for example, have LREE-enriched patterns, high LREE/HFSE ratios (Fig. 1), and high initial ε_{Nd}^{143} (Harper et al., 1995; Jagoutz, 1996) Thus, whereas the Nd isotope systematics of the Nakhlites are indicative of derivation from source regions with strong time-integrated LREE depletions, the LREE enrichment of the melts suggest derivation from LREE-enriched sources. To explain this seeming contradiction, the REE systematics of the Nakhlites have generally been attributed to very small degrees of melting of a previously depleted source (e.g., Nakamura et al., 1982; Longhi, 1991). In contrast to the nakhlites, the shergottites have LREE-depleted patterns, low LREE/HFSE ratios (Fig. 1), and relatively low initial ε_{Nd}^{143}. Thus, the compositions of the shergottites are essentially complementary to the nakhlites. In order to account for the strong LREE depletions in the shergottites, many authors have suggested that their mantle sources were previously melted and initially contained garnet (e.g., Nakamura et al., 1982; Longhi, 1991; Longhi et al., 1992; Gleason et al., 1996).

Calculated major-element compositions of the shergottite parent magmas have lower Al_2O_3 (3-12.5 wt. %) than typical terrestrial basalts (Stolper and McSween, 1979; Treiman, 1986; Longhi and Pan, 1988; Johnson et al., 1991), which is consistent with derivation from a previously depleted source (Longhi, 1991). However, pseudo-ternary projections of SNC parent-magma compositions into systems with diopside-orthopyroxene-olivine-and an aluminous phase (plagioclase-spinel-garnet between 5-35 kb pressure) demonstrate that the parent magmas have Al abundances that are too low to be in equilibrium with any aluminous phase and, therefore, cannot be derived from source regions that contain garnet (Longhi, 1991). The apparent contradiction between the presence of garnet in the sources on one hand, and low abundances of Al in the magmas (which prevent equilibration of the magmas with garnet) on the other, have been attributed

to 1) removal of garnet by late stage melting events (Gleason et al., 1996), or 2) mixing between melts derived from garnet-bearing sources at high pressure and melts derived from garnet-free sources at lower pressure (Longhi, 1991).

The Rb-Sr and Sm-Nd isotopic systematics of SNC meteorites help to constrain their petrogenetic relationships. Shih et al. (1982) noted that the whole rock Rb-Sr of the SNC meteorites fell on a 4.5 Ga reference isochron, whereas the whole rock Sm-Nd data of the shergottites defined an isochron with a slope corresponding to an age of ~1.3 Ga. This ~1.3 Ga shergottite whole rock isochron has been interpreted in varying ways. Shih et al. (1982) suggested that the 1.3 Ga whole rock age likely approximated the common crystallization age of the shergottites. This was supported by 1) discordant Rb-Sr and Sm-Nd internal isochron and $^{40}Ar/^{39}Ar$ ages for the shergottites that indicated the systems had been reset by open-system processes, 2) 1.3 Ga crystallization ages determined on the nakhlites, that indicated melting processes were occurring on the SNC parent body at this time, and 3) the generally complementary trace-element abundance patterns of nakhlites and shergottites. Measured Rb-Sr and, in some cases, Sm-Nd internal isochron ages of ~180 Ma were, therefore, interpreted to reflect resetting of the isotopic systems by events and processes accompanying shock metamorphism.

Jones (1986, 1989) and Jagoutz (1991) offered an alternative hypothesis in which they suggested that the 1.3 Ga and 4.5 Ga whole rock "isochrons" were actually mixing lines between various mantle and crustal reservoirs. This conclusion was based on 1) the difficulty of resetting Rb-Sr and Sm-Nd isotopic systems by shock metamorphism, 2) preservation of primary igneous zoning patterns in the major mineral phases, and 3) the observation that initial Sr, Nd, and Pb isotopic compositions of the shergottites calculated at 180 Ma lie on or close to an apparent mixing plane. In the Jones (1989) model, neither the 4.5 Ga Rb-Sr nor the 1.3 Ga Sm-Nd whole-rock isochron are given any age significance. In the Jagoutz (1991) model, the 4.5 Ga Rb-Sr whole rock isochron is interpreted as the age of initial crust-mantle differentiation, whereas the 1.3 Ga Sm-Nd isochron is simply a mixing line. The various models not withstanding, the similarity in bulk Rb-Sr and Sm-Nd isotopic systematics in a group of rocks presumably sampled from various

localities on Mars is puzzling. We feel that any petrogenetic model for the origin of the SNC meteorites must account for both the ~4.5 Ga Rb-Sr and the ~1.3 Ga Sm-Nd whole rock isochrons, as well as define the open-system processes potentially responsible for the discordant Rb-Sr and Sm-Nd internal-isochron ages. The model presented later in this paper attains considerable success in reproducing the Sr and Nd isotopic evolution of many of the SNC meteorites.

ANALYTICAL TECHNIQUES

The mineral separation procedure for QUE 94201 is presented in Fig. 2. A 330 mg split of QUE 94201,31 was crushed with a boron carbide mortar and pestle. Two 15.3 and 52.5 mg splits (WR-1 and WR-2) were set aside for whole-rock isotopic analysis, and the remainder was sieved at 74-150 μm (100-200 mesh) and 44-74 μm (200-325 mesh). The fine size fraction (44-74 μm) was leached in warm 1N HCl for 10 minutes yielding a whole-rock leachate (WR-L) and a residue from which mineral fractions were subsequently separated (leachates and residues are hereafter designated by L and R). Maskelynite (Plag-1R) and bulk pyroxene (Pyx-R) separates from the residue of the fine size fraction were concentrated using heavy liquids with densities of 2.65 and 3.32-4.05 g/cm^3, respectively. Each separate was washed to remove heavy liquids and further purified (>99.5%) by hand-picking. Composite grains of glass (~80%) and pyroxene (~20%) separated from the Pyx-R fraction by hand-picking were designated Glass-1R.

Maskelynite (Plag-2), high-Fe pyroxene (Fe-Pyx-R), and high-Mg pyroxene (Mg-Pyx-R) were separated from the course size fraction (74-150 μm) using a Frantz magnetic separator. These separates were further hand-picked and, like those from the fine size fraction, were extremely pure (>99.5%). The Fe-Pyx-R and Mg-Pyx-R, as well as a third plagioclase separate (Plag-3), that was transferred to D. Bogard for $^{40}Ar/^{39}Ar$ analysis, were leached in warm 1N HCl prior to digestion yielding leachates Fe-Pyx-L, Mg-Pyx-L, and Plag-3L. A second mixed glass (~65%) and pyroxene (~35%) separate (Glass-2) was generated by hand-picking the Fe-Pyx and Mg-Pyx fractions prior to leaching. The Plag-2 and Glass-2 separates were not leached.

The whole rocks and mineral separates were digested in HF-HNO_3 acids. Rb-Sr and Sm-Nd concentrations were run on small splits of each mineral fraction and leachate to insure correct spike/sample ratios. The WR-2 split was run to search for a radiogenic ^{142}Nd enrichment and was not spiked with the mixed ^{149}Sm-^{150}Nd spike used for the other samples. Cations were separated using cation specific resins and micro columns as follows: Sr was separated using Bio-Rad Sr-spec resin (50-100μm bead size) with 3N HNO_3 acid and quartz-distilled water; Rb was separated and Fe removed from REE using AG50X12 resin with 2N HCl, REE were eluted in 6N HNO_3; REE were purified using Bio-Rad REE resin (50-100μm bead size) with 1N HNO_3 and 0.05N HNO_3 acids, and Sm and Nd were separated using a AG50X8 (NH_4 form) and α-hydroxyisobutyric acid (α-HIBA). Complete procedural blanks (pg) were 11-15 for Rb, 25-38 for Sr, 4-7 for Sm, and 22-25 for Nd. The 52.5 mg WR-2 sample was put through the α-HIBA separation procedure twice, in order to insure good separation of ^{142}Ce from Nd, and had a blank contribution of about 35 pg. All samples were run statically on a multi-collector Finnigan MAT 261 mass spectrometer. Sr was loaded on Re filaments with Ta_2O_5 + H_3PO_4. Nd was run on single and double Re filaments as an oxide and as a metal, respectively. Run conditions, error calculations, and values for standards are presented in Tables 1 and 2.

RESULTS

Rb-Sr and Sm-Nd isotopic analyses on mineral fractions, whole rocks, and leachates determine the age of crystallization, the initial isotopic composition, and the presence of a ^{142}Nd anomaly (Tables 1, 2). These analyses also allow us to assess the effects that the addition of secondary sulfate and phosphate phases might have on the isotopic systematics of the sample. The results are presented below.

Rb-Sr and Sm-Nd isochrons

A Rb-Sr isochron giving an age of 327±12 Ma is defined by three pyroxene (Pyx-R, Fe-Pyx-R, and Mg-Pyx-R), two maskelynite (Plag-1R and Plag-2) mineral fractions, and the WR-2

split (Fig. 3). Although this age is about 150 Ma older than the Rb-Sr ages of the other shergottite meteorites (e.g., Nyquist et al., 1979; Shih et al., 1982; Jagoutz, 1989; Nyquist et al., 1995a), it is roughly similar to the age for Shergotty (360 Ma) reported by Jagoutz and Wänke (1986). It is important to note, however, that our Rb-Sr age for QUE 94201 is based solely on the analyses of major mineral residues (and one whole rock) from which potential contaminants were removed by leaching in HCl, whereas the Shergotty age was derived from analyses of both mineral fractions and leachates (Jagoutz and Wänke, 1986). Our Rb-Sr age is, therefore, less likely to be affected by the post-crystallization addition of leachable secondary components, such as sulfates or phosphates.

The leachates WR-L, Mg-Pyx-L, and Fe-Pyx-L fall off the 327 Ma isochron, indicating that the whole rock contains a leachable fraction that is not in isotopic equilibrium with the silicate mineral fractions (Fig. 3). This component appears to be detectable in the unleached WR-1 and Glass-2 fractions as well, which like the leachates, fall above and to the left of the 327 Ma isochron defined by the residues. Thus, this added component has high $^{87}Sr/^{86}Sr$, but low $^{87}Rb/^{86}Sr$. Both Ca sulfates and phosphates are easily leachable secondary phases observed in QUE 94201 (Harvey et al., 1996; Wentworth and Gooding, 1996), that may have high Sr abundances, low Rb/Sr ratios, and likely contain radiogenic "crustal" Sr that could raise the $^{87}Sr/^{86}Sr$ ratios of WR-1 and the leachates. The Plag-3L and Glass-1 fractions also lie slightly off the isochron (to the right), but unlike the other leachates cannot be explained by the addition of a high $^{87}Sr/^{86}Sr$ component. These fractions have low abundances of Sr (7 and 19 ng, respectively) and Rb (0.02 and 2.6 ng, respectively), and may be subject to expanded analytical uncertainty resulting either from blank contributions or decreased precision of the mass spectrometer runs.

A Sm-Nd age of 327±19 Ma (Fig. 4) is defined by the relatively REE-enriched mineral fractions and leachates (Mg-Pyx-R, Fe-Pyx-R, WR-1, and WR-L splits). This Sm-Nd age is concordant with the Rb-Sr age, although the two isochrons are defined by different fractions of the sample. The relatively REE-depleted mineral fractions and leachates (Plag-1R, Plag-2, Plag-3L,

Pyx-R, Mg-Pyx-L, Fe-Pyx-L, Glass-1R and Glass-2) fall to the left and below the 327 Ma Sm-Nd isochron.

In order to better understand the Sm-Nd systematics of QUE 94201 mineral fractions and leachates, and determine why concordant Rb-Sr and Sm-Nd ages are given by isochrons defined by different mineral fractions, the abundances of Sm and Nd in the mineral fractions are compared with the in situ ion microprobe analyses of McSween et al. (1996) and Wadwa and Crozaz (1996) in Fig. 5. The concentrations of Nd and Sm determined by isotope dilution for the pyroxene mineral separates, Fe-Pyx-R and Mg-Pyx-R, are similar to the ion microprobe data for pyroxene, and are therefore consistent with the observation that the Sm and Nd in these fractions reflect trace-element partitioning during igneous crystallization. Similarly, the abundances of Sm and Nd measured in WR-L by isotopic dilution are very similar to those measured in whitlockite by ion microprobe, suggesting that REE abundances in WR-L are dominated by the igneous whitlockite component. This is reasonable given the high solubility of whitlockite in the 1N HCl used to leach the whole rock and the high modal abundance of whitlockite in QUE 94201. Thus, the position of the WR-L datum on the 327 Ma Sm-Nd isochron is also likely to reflect trace-element partitioning during igneous crystallization. The bulk WR-1 split falls near the 327 Ma isochron, probably as a result of the dominance of the whole rock REE abundances by the whitlockite component (Wadwa and Crozaz, 1996). The impact melt Glass-2, and the leachates Mg-Pyx-L and Fe-Pyx-L have $^{147}Sm/^{144}Nd$ and $^{143}Nd/^{144}Nd$ values that are similar to those of the WR-L and WR-1 fractions, suggesting that they also contain a large whitlockite component. However, these fractions, particularly the pyroxene leachates, are displaced slightly from the position of a "pure" whitlockite component in the isochron diagram, suggesting the possible presence of one or more additional components.

In contrast to the abundances of Sm and Nd in the pyroxene, whole rock, and whole rock leachate (whitlockite?) fractions, the Sm and Nd isotope dilution measurements of the Plag-1R, Plag-2, and Plag 3L fractions are significantly different from the ion microprobe data (Fig. 5). The unleached Plag-2 separate has much higher abundances of Sm and Nd, and a much lower ratio of

Sm/Nd than the ion microprobe values for maskelynite. Similar $^{147}Sm/^{144}Nd$ and $^{143}Nd/^{144}Nd$ ratios and even higher Sm and Nd abundances were measured in Plag-3L (Table 2; Fig. 5), suggesting that the plagioclase fractions contain a leachable component characterized by lower $^{147}Sm/^{144}Nd$ and $^{143}Nd/^{144}Nd$ than found in any of the igneous minerals that were analyzed by ion microprobe. The high REE abundances in Plag-1R compared to those in maskelynite (Fig. 5) suggests that it also contains one or more extraneous REE components, despite the fact that it was leached. One potential explanation is that small amounts of extraneous components, such as shock-produced melts of pyroxene, phosphate, and/or secondary alteration products were added to the maskelynite during its formation by shock metamorphism. Although such a melt component is likely to be present to some degree in all the phases analyzed (e.g., McKay et al., 1996), it is expected to most strongly affect the REE systematics of maskelynite because this phase contains the lowest REE abundances of any primary igneous mineral analyzed in this study.

Thus, analysis of mineral fractions and leachates in QUE 94201 demonstrate the presence of a leachable component that is distinct from the primary igneous phosphate and is not in isotopic equilibrium with the primary mineral phases. This component is characterized by high $^{87}Sr/^{86}Sr$ and low $^{147}Sm/^{144}Nd$ and $^{143}Nd/^{144}Nd$ indicating that it is derived from a crustal source. In addition, this component has low $^{87}Rb/^{86}Sr$ suggesting that its source is one or more secondary minerals enriched in alkaline earth elements, such as Ca sulfates and phosphates that have been observed in QUE 94201 by Wentworth and Gooding (1996). The observation that the host phases are easily leachable suggests that they are present on grain surfaces and is consistent with secondary alteration of the rock by crustal fluids. The addition of this secondary component to various mineral fractions may explain the discordant ages derived from the Rb-Sr and Sm-Nd systems for many SNC meteorites.

Although the Sm-Nd systematics of the plagioclase fractions are strongly affected by the presence of leachable alteration products, their Rb-Sr systematics are unaffected. This probably reflects the large amount of Sr in the plagioclase fraction relative to the amount of Sr added from secondary components. Thus, the addition of secondary alteration products to QUE 94201 has

varying effects on the Rb-Sr and Sm-Nd systematics of the different mineral fractions. The presence of secondary alteration products enriched in alkaline and rare earth elements 1) can affect the Sm-Nd, but not the Rb-Sr systematics of the plagioclases, 2) can affect the Rb-Sr, but not the Sm-Nd systematics of the whole rock and whole rock leachates, and 3) does not appear to affect either the Rb-Sr or the Sm-Nd systematics of the pyroxenes within detection limits. The susceptibility of particular mineral fractions to isotopic perturbation through the addition of alteration products is probably determined by a combination of the robustness of the phase that comprises the mineral separate (i.e. resistance of the phase to chemical alteration) and the concentrations of Rb, Sr, Sm, and Nd in the phase relative to their concentrations in the alteration products.

Jagoutz and Wänke (1986) measured pyroxene leachates with $^{147}Sm/^{144}Nd$ and $^{143}Nd/^{144}Nd$ ratios that are similar to the values we measured for Plag-2, Plag-3L, and Glass-1R fractions, and interpreted their leaches to be derived from a primary igneous component. As discussed above, leachable components with low $^{147}Sm/^{144}Nd$ and $^{143}Nd/^{144}Nd$ observed in QUE 94201 are unlikely to be a primary igneous component, however. In the Rb-Sr system (Fig. 3) the leachates define a line that has a slope corresponding to an age of about 4.2 Ga, whereas in the Sm-Nd system (Fig. 4) the same fractions define a line that has a slope corresponding to an age of about 1.1 Ga. This suggests that the leachates are in fact mixtures derived from both primary (mantle) and secondary (crustal) sources. The fact that the leachates define mixing lines that are sub-parallel to the Rb-Sr and Sm-Nd whole rock isochrons previously determined for SNC meteorites suggests that the added "crustal" material is likely to be of Martian, rather than terrestrial, origin.

In summary, the concordant Rb-Sr and Sm-Nd isochron ages of 327 Ma determined from primary mineral phases clearly give the crystallization age of QUE 94201. Nevertheless, there are at least two leachable components in QUE 94201. The first leachable component is whitlockite which dominates the REE systematics of whole rock and pyroxene leachates. The other leachable component is derived from secondary alteration products that adhere to grain surfaces. Although

this component affects all the leachates to some degree, it is most prevalent in the Rb-Sr systematics of the pyroxene leachates and the Sm-Nd systematics of the plagioclase leachates. The presence of secondary alteration products in some of the leachates does not alter the fundamental conclusion that the crystallization age of QUE 94201 is 327 Ma.

Initial Sr and Nd isotopic ratios and ^{142}Nd excess

The Rb-Sr isochron defines an initial $^{87}Sr/^{86}Sr$ of 0.701298±14 (Fig. 3). This value is essentially the same as that measured in the Plag-1R, Plag-2, and Plag-3L fractions (Table 1) because of their very low $^{87}Rb/^{86}Sr$, and the relatively young crystallization age of the sample. This is the lowest initial $^{87}Sr/^{86}Sr$ yet measured for any of the SNC meteorites (next lowest initial $^{87}Sr/^{86}Sr$ = 0.70494 for Governador Valadares calculated at 327 Ma; Wooden et al., 1979), indicating that QUE 94201 is derived from a Martian source with the strongest time-integrated depletion of Rb relative to Sr of which we have record (Borg et al., 1996). Initial ε_{Nd}^{143} determined from the 327 Ma isochron is +47.6±1.7 (Fig. 4). This value is dramatically higher than for any of the other SNC meteorites (next highest initial ε_{Nd}^{143} is +28.4 calculated for ALH 84001 at 327 Ma; data from Nyquist et al., 1995a), but is consistent with the very high whole rock $^{147}Sm/^{144}Nd$ of 0.503 (Table 2). Such low $^{87}Sr/^{86}Sr$ and high ε_{Nd}^{143} and $^{147}Sm/^{144}Nd$ values indicate 1) that QUE 94201 was derived from a source that was strongly depleted in $^{87}Rb/^{86}Sr$ and enriched in $^{147}Sm/^{144}Nd$ during most of its history, and 2) the QUE 94201 parent magma could have assimilated only a small amount of incompatible-element enriched crustal material. Nevertheless, there is evidence (presented in a later section) to suggest that QUE 94201 may have assimilated a small amount of Martian crustal material, so that its initial $^{87}Sr/^{86}Sr$ value also may represent a mixture of mantle and crustal components.

We analyzed several bulk samples and leachates in search of a ^{142}Nd anomaly that would constrain the time at which the QUE 94201 source was initially depleted in LREE. Excess ^{142}Nd would be produced from an enrichment of Sm (in particular the now extinct nuclide ^{146}Sm) over Nd relative to the chondritic Sm/Nd ratio in the restite during partial melting occurring soon after condensation of Martian materials from the solar nebula ($t_{1/2}$ of ^{146}Sm is 103 Ma). Comparatively

large ^{142}Nd anomalies were found for several whole rocks and leachates (ε_{Nd}^{142} = +0.8 to +0.99; unspiked whole rock = +0.92±0.11) and are indicative of very early and very efficient fractionation of Sm from Nd. The ε_{Nd}^{142} anomaly observed in QUE 94201 is similar in magnitude to the largest ε_{Nd}^{142} anomaly observed in the Nakhlites and Chassigny (Harper et al., 1995; Jagoutz, 1996), and suggests that the sources of these samples experienced similar early differentiation events.

A model age for the depletion event can be calculated using the techniques outlined in Nyquist et al. (1995b), and by assuming $^{147}Sm/^{144}Nd$ ratios for the early-depleted Martian mantle. Harper et al. (1995), for example, suggested that the ε_{Nd}^{142} of +0.59±0.13 observed in Nakhla could be produced by differentiation occurring at 4539 Ma assuming $^{147}Sm/^{144}Nd$ = 0.235 of the Nakhla source (e.g., Jones, 1989; Harper et al., 1995) using the equation:

$$\varepsilon_{Nd}^{142} = 354(^{146}Sm/^{144}Sm)(f^{Sm/Nd})e^{-\lambda_{146}(\Delta t)}$$

where $f^{Sm/Nd}$ is the fractionation factor defined by $[(^{147}Sm/^{144}Nd)_R/(^{147}Sm/^{144}Nd)_{CHUR} - 1]$, λ_{146} is 0.00673, $^{146}Sm/^{144}Sm$ is 0.008 (we use 0.0076; e.g., Nyquist et al., 1995b), and Δt is the time interval between solar system condensation at 4566 Ma (we use the 4558 Ma Pb-Pb age of angrite LEW 86010 of Galer and Lugmair, 1992) and differentiation that produced the depleted mantle source.

The very high ε_{Nd}^{142} observed in QUE 94201 is not consistent with derivation from a Nakhla-like source with $^{147}Sm/^{144}Nd$ values near 0.235. In fact, $^{147}Sm/^{144}Nd$ values in excess of 0.264 are required to obtain positive model ages from ε_{Nd}^{142} of 0.92. Indeed, Harper et al. (1995) were also unable to generate positive ages using both $^{147}Sm/^{144}Nd$ of 0.235 and the mean measured ε_{Nd}^{142} value, and were forced to use the lowest limit of measured ε_{Nd}^{142} values (i.e. +0.46) in order to obtain a positive age. If the lower limit of the QUE 94201 ε_{Nd}^{142} values are used (i.e. +0.82) then $^{147}Sm/^{144}Nd$ of 0.257 is required to yield positive model ages. The $^{147}Sm/^{144}Nd$ ratios calculated from the ε_{Nd}^{142} data represent the minimum values, because the differentiation is assumed to occur immediately after formation of the earliest solids in the solar system. Nevertheless, calculated $^{147}Sm/^{144}Nd$ ratios in excess of 0.25 indicate that the QUE

94201 source had to be strongly fractionated from the CHUR value of 0.1967 very early in Martian history. If the QUE 94201 source was not differentiated until 100 Ma after solar condensation, for example, then the source must have an even higher $^{147}Sm/^{144}Nd$ value (> 0.313) to produce $\varepsilon_{Nd}{}^{142}$ of +0.82. Potential Martian mantle sources with such high $^{147}Sm/^{144}Nd$ values are similar to the most depleted lunar sources postulated to exist at 4.4 to 4.5 Ga by Misawa et al. (1993) and Snyder et al. (1994) and inferred from the ^{142}Nd data of lunar basalts (Nyquist et al., 1995b). Thus, mantle differentiation of Mars must have been very early and very extreme.

MODELING Nd AND Sr ISOTOPIC EVOLUTION IN THE MARTIAN MANTLE

We have constructed time-integrated non-modal partial melting models to constrain 1) the petrogenesis of QUE 94201, 2) the timing of potential depletion events in the QUE 94201 mantle source region, 3) the isotopic composition of potential Martian mantle and crustal reservoirs, and 4) the relationships between QUE 94201 and the other shergottites. The assumptions required to construct the models are first outlined and then the models are presented.

Composition of sources

The partial-melting models attempt to reproduce the Sm-Nd and Rb-Sr isotopic compositions of QUE 94201 through a series of partial melting events of primitive (chondritic) Martian mantle beginning 4.558 Ga ago. The initial composition of the primitive Martian mantle is assumed to have Sm and Nd in 2xC1 chondrite abundances (values of Sun and McDonough, 1989) as per Gleason et al. (1996) and $^{147}Sm/^{144}Nd = 0.1967$. The concentration of Rb in the Martian mantle is difficult to estimate given its volatile nature and the predicted relative abundance of volatiles on Mars (e.g., Dreibus and Wänke, 1985). We have calculated a $^{87}Rb/^{86}Sr$ value of 0.16 for bulk silicate Mars using Rb/Ca and Sr/Ca estimated for Mars and Earth, respectively, from data of Jagoutz et al. (1979), Wänke and Dreibus (1988), and Longhi et al. (1992), assuming that Sr/Ca is the same for the Earth and Mars. Since Sr is a moderately refractory element, we have assumed that Sr = 2xC1 (14.5 ppm), so that Rb = 0.82 ppm assuming the Rb/Sr ratio above. Although the concentration of Rb is about 20% lower than the estimated abundance for crust +

mantle by Longhi et al. (1992), this lower value is consistent with estimated abundances of Sm and Nd in primitive Martian mantle that are derived from 2xC1 values.

Since the modal mineralogy of the mantle is poorly constrained, we have used modes that are consistent with estimates of major-element abundances in bulk crust-mantle. The modal mineralogy of the undifferentiated source is based on the model major element composition of mantle + crust of Longhi et al. (1992), which corresponds to Ol:Opx:Cpx:Gar = 60:17:10:13. Although the abundance of Al in QUE 94201 is too low for the magma to be in equilibrium with garnet, very high $^{147}Sm/^{144}Nd$ of the whole rock require the presence of a phase, such as garnet, that can substantially fraction Sm from Nd (Gleason et al., 1996). As mentioned earlier, low Al in parental magmas may reflect exhaustion of garnet during the last melting event, or re-equilibration of magmas produced from garnet-bearing peridotites with garnet-free peridotites in a polybaric melting scheme (as per Longhi, 1991). The melt proportions assumed for the modeling is Ol:Opx:Cpx:Gar = 31:19:27:23, and are roughly consistent with estimated shergottite parent magma compositions (e.g., Longhi and Pan, 1989). Note that repeated melting of the same source in these proportions will deplete the source in garnet and clinopyroxene, and enrich it in olivine.

Although we have attempted to make phase proportions used in our models consistent with estimates of major element abundances in bulk silicate Mars, Rb and Sr are relatively unaffected by the proportions of phases in the source, as well as in the melt assemblage, because of their incompatibility in all phases considered (Table 3). Likewise, only the proportions of garnet in the source and in the melt assemblage will effect the Sm and Nd abundances in the modeled melts (Table 3). Thus, the critical factors controlling the distribution of Rb-Sr and Sm-Nd, and the isotopic systematics of the melt and restite in the models are 1) the number of melting events the source has undergone, 2) the degree of melting of each event, 3) the proportions of garnet in the restite (in the case of Sm-Nd), and 4) the timing of the melt events.

Number and timing of melting events

Incompatible element, REE, and isotopic systematics of QUE 94201 provide evidence for numerous and early melting events in the QUE 94201 source region. The low abundances of

incompatible elements and low LREE/HREE ratios indicate that QUE 94201 was derived from a source that was previously melted because such strong depletions are not consistent with a single melting event. Instead the QUE 94201 source is likely to have undergone numerous episodes of melting. The 327 Ma crystallization age of QUE 94201 is indicative of a recent melting event which would have depleted its source, whereas the high $^{143}Nd/^{144}Nd$ and low initial $^{87}Sr/^{86}Sr$ of QUE 94201 indicate that the source was depleted in Rb/Sr and enriched in Sm/Nd early in geologic history, long before the formation of QUE 94201. Furthermore, the presence of excess ^{142}Nd in QUE 94201 requires that some depletion of its mantle source occurred very early in the history of the planet, and like the Nakhlite source, was probably associated with an initial crust forming event (Harper et al., 1995; Shih et al., 1996).

Our modeling indicates that in order to produce the $^{147}Sm/^{144}Nd$ observed in QUE 94201 using modal mineralogy outlined above, at least three episodes of partial melting (each of about 7%) are required. However, models that use only three episodes of melting fail to approximate the abundances of Nd and Sm of QUE 94201 (modeled Nd = 0.65 ppm and Sm = 0.55 ppm compared to measured values of Nd = 1.5 ppm and Sm = 1.2 ppm). Furthermore, the Nd isotopic systematics of QUE 94201 are not reproduced by this model no matter when the three melting events are assumed to occur. For example, in order to produce the observed ε_{Nd}^{142} of QUE 94201, the first melting event must occur at 4.43 Ga yielding a restite with $^{147}Sm/^{144}Nd$ of 0.356. Such a restite is an unrealistic source for QUE 94201 because at the time of QUE 94201 magma extraction it has ε_{Nd}^{143} of +84.6, which is roughly double the calculated initial ε_{Nd}^{143} of QUE 94201. A greater number of less extensive melting events are therefore required. Similar arguments can be used to eliminate models that employ only four episodes of melting because such models require that the QUE 94201 source has ε_{Nd}^{143} of +62.6 at the time of magma extraction.

The simplest model that can account for both the ε_{Nd}^{142} and ε_{Nd}^{143} of QUE 94201 requires five episodes of melting. The first two melts are removed from the source early in the history of the planet around 4.5 Ga, and the other three are removed around 327 Ma. It follows that the isotopic systematics of the modeled melts are completely determined by the early melting events

(since source depletions occurring at the time of crystallization will not alter the isotopic composition of the source), whereas the $^{147}Sm/^{144}Nd$ and Nd and Sm concentrations of the modeled melts are determined by all of the melting events. Although repeated melting events occurring at approximately evenly space intervals of time would seem more in keeping with a continuously active planet such as the Earth or Mars, it is not consistent with the Nd isotopic data. This stems from the fact that in order to produce the ε_{Nd}^{142} anomaly of +0.92 the source must be strongly depleted early in its history. Any subsequent melting that occurs must be fairly late (i.e. near 327 Ma) otherwise the $^{147}Sm/^{144}Nd$ of the source is raised while there is still time for ^{143}Nd to be produced by the decay of ^{147}Sm. The end result is a melt with ε_{Nd}^{142} of +0.92, but ε_{Nd}^{143} that is too high. For example, assuming an intermediate melting event at about 300 Ma before QUE 94201 melt extraction (i.e. 625 Ma ago) raises the modeled initial ε_{Nd}^{143} to +64. We therefore assume that the QUE 94201 source has undergone only two periods of melting; one that occurred early in the history of the planet around 4.5 Ga ago and the other that occurred at 327 Ma.

Partial melting models

The results of our most reasonable Sm-Nd-based partial melting model is presented in Fig. 6 and Table 4 (see the figure caption for detailed model parameters). One percent melting of a chondritic source at 4.525 Ga produces a depleted source with $^{147}Sm/^{144}Nd$ of 0.234 (and ε_{Nd}^{142} of +0.41) and a melt with very low $^{147}Sm/^{144}Nd$ (0.097). This melt represents an extremely fractionated early-formed crust (crust #1), and has a present day ε_{Nd}^{143} value that is near -59. In the model, the depleted source is immediately melted again (1%), producing a source with $^{147}Sm/^{144}Nd$ of 0.281 (and ultimately a ε_{Nd}^{142} value of +0.92). The source is not melted again until 327 Ma, when it undergoes three episodes of melting. The third and fourth episodes of partial melting (4%) at 327 Ma produce the QUE 94201 source. The final (fifth) melting event (4%) at 327 Ma generates a melt with Nd and Sm concentrations, $^{147}Sm/^{144}Nd$, ε_{Nd}^{143}, and ε_{Nd}^{142} values that are similar to QUE 94201 (Table 4).

In summary, the Sm-Nd isotopic systematics of QUE 94201 can be reproduced from a chondritic source by five episodes of melting; two at 4.525 Ga, and three at 327 Ma. The timing

of the first two melting events is fixed by the assumption that QUE 94201 is derived from a single source that initially had a chondritic $^{147}Sm/^{144}Nd$ ratio and that subsequent depletions occurred at 327 Ma. If initial melting occurred later than 4.525 Ga, then the source is required to have a $^{147}Sm/^{144}Nd$ ratio that is higher than 0.281 to produce the observed ε_{Nd}^{142} anomaly. However, a source with $^{147}Sm/^{144}Nd$ ratio that is greater than 0.281 will yield melts at 327 Ma that have higher initial ε_{Nd}^{143} values than QUE 94201. Thus, melting must occur at or before 4.525 Ga ago if QUE 94201 is produced by five episodes of melting as outlined above.

We have varied several of the model parameters in order to discern consistent model results that are independent of the initial assumptions employed in the models. The parameters we have varied include the melt proportions at each melting episode and the amount of garnet in the source. The effects of less than five episodes of melting are discussed above. The model outlined above requires the amount of partial melting to increase with time. Intuitively, one expects the opposite to occur, that is, for the amount of partial melting to decrease, or at least stay about the same with time. Models that assume constant amounts of melting are able to generate a melt with the $^{147}Sm/^{144}Nd$ ratio, and Sm and Nd concentrations that are similar to QUE 94201 in five melt episodes of about 2% each. In order to produce the observed ε_{Nd}^{142}, this model requires the initial two melting events (events #1 and #2) to occur at 4.395 Ga. The timing of the initial two melting events calculated by this model are 130 Ma later than in our best model, in which the initial melts are of smaller volume (2% melting compared to 1% melting), because the $^{147}Sm/^{144}Nd$ of the restite increases with larger degrees of melting as a result of mass balance. This model is unsuccessful, however, because the initial melting events produce a source that has a $^{147}Sm/^{144}Nd$ ratio that is too high, resulting in an initial ε_{Nd}^{143} of QUE 94201 that is also too high (+106). Thus, to reproduce both the ε_{Nd}^{143} and ε_{Nd}^{142} values of QUE 94201 the early melt events must be relatively small volume compared to the later events.

In our best model, outlined in Fig. 6, the source is assumed to have about 13 percent garnet. This results in a $^{147}Sm/^{144}Nd$ ratio of the QUE 94201 restite (Mantle #5) that is extremely high (1.24). If less garnet is assumed in the restite assemblage, then the $^{147}Sm/^{144}Nd$ of the

source would be lower, although it becomes increasingly difficult to produce both the $^{147}Sm/^{144}Nd$ and Nd and Sm concentrations observed in QUE 94201 as the amount of garnet in the source decreases. For example, if the source is assumed to contain no garnet, then a modeled melt with $^{147}Sm/^{144}Nd$ of QUE 94201 can be produced by five episodes of melting (each about 7%; the first two melting events occur at 4.500 Ga and the last three at 327 Ma) of a source with Ol:Opx:Cpx = 40:30:30 that is melted in the proportions Ol:Opx:Cpx = 10:30:60. The modeled $^{147}Sm/^{144}Nd$ of QUE 94201 restite (Mantle #5) is down to 0.68, and the calculated initial ε_{Nd}^{143} is +54 (compared to the measured ε_{Nd}^{143} of QUE 94201 which is +47.6). Although the major-element composition of this modeled source is unlike Longhi's (1992) estimates for bulk silicate Mars, the most significant failure of the model is in reproducing the Sm and Nd concentrations of QUE 94201 (calculated values for Nd and Sm are 0.13 ppm and 0.11 ppm compared to measured values of 1.5 ppm and 1.2 ppm). Thus, although our best model presented in Fig 6 is not completely satisfactory because it has small percentages of melting early in the history of the planet and leaves a restite with very high $^{147}Sm/^{144}Nd$, it best reproduces the geochemical and Nd-isotopic measurements of QUE 94201.

There are two important consistencies among all of the models, which emphasize key geologic processes on Mars. First, initial differentiation of Mars must have occurred very early in order to produce both the ^{142}Nd and ^{143}Nd systematics of QUE 94201 from a single source. Our best estimate is that initial differentiation occurred on or before 4.525 Ga (at about 33 Ma after planet formation), although ages as late as 58 Ma and 163 Ma can also be derived from garnet-free and constant melt volume models discussed above. Second, there had to be a long period of relatively little activity between 4.5 Ga and 327 Ma in which only trivial amounts of melt were extracted from the QUE 94201 source. Large amounts of melting occurring between 4.5 Ga and 327 Ma raise $^{147}Sm/^{144}Nd$ of the source so that ε_{Nd}^{143} becomes higher than the measured initial ε_{Nd}^{143} value. Thus, the QUE 94201 source is likely to have remained fairly isolated since initial differentiation of the planet.

Rb-Sr-based partial melting models are not able to reproduce the Rb-Sr systematics of QUE 94201 using the same source mineralogy, melt proportions, degrees of melting, and number of melting events as used for the Sm-Nd based models. This stems from the fact that the modeled mantle is virtually depleted in Rb after only a few episodes of melting. For example, the modeled mantle has $^{87}Rb/^{86}Sr = 0.02$ after one melt extraction, and $^{87}Rb/^{86}Sr = 3x10^{-7}$ after five melt extractions, so that $^{87}Sr/^{86}Sr$ does not evolve past a value of 0.700 (Table 4). The fact that initial $^{87}Sr/^{86}Sr$ values of all of the SNC meteorites are higher than 0.700 (e.g., Nyquist et al., 1979; Shih et al., 1982; Jagoutz, 1989; Nyquist et al., 1995a), suggests that they cannot be produced directly from the modeled mantle. More radiogenic initial $^{87}Sr/^{86}Sr$ values will result if a primitive Martian mantle $^{87}Rb/^{86}Sr$ value that is higher than 0.16 is assumed. However, to produce a melt with an initial $^{87}Sr/^{86}Sr$ value similar to QUE 94201, the $^{87}Rb/^{86}Sr$ of the primitive mantle must be about 5 times higher than 0.16. Such high Rb abundances are not reasonable, and suggest that the Rb-Sr systematics of QUE 94201 (and the other SNC meteorites) are not controlled by mantle melting processes alone.

DISCUSSION

The Sm-Nd data suggest that QUE 94201 is produced by multiple melting events that began soon after condensation of Mars from the solar nebula, whereas the Rb-Sr data suggest that QUE 94201 was derived from a source that had not undergone multiple melting events. To investigate these discrepancies between the Rb-Sr and Sm-Nd systematics, the isotopic compositions of all the SNC meteorites, as well as the potential crustal and mantle reservoirs calculated by the models are compared. In this section, the constraints the partial melting models offer on the formation age and composition of Martian mantle and crustal reservoirs is explored, and a simple petrogenetic model for the origin of the shergottites is proposed.

Petrogenesis of shergottites: Evidence of mixing

Figure 7 is a $^{147}Sm/^{144}Nd$ vs. $^{143}Nd/^{144}Nd$ isochron plot of shergottite initial whole rock values (recalculated for an average age of the shergottites at 180 Ma). Also shown on this plot are

the compositions of representative crustal and mantle reservoirs (at 180 Ma) derived from the partial melting models developed in the previous section. Crust #1, crust #2, and crust #3 are the first, second, and third melts extracted from the initial chondritic source at 4.525 Ga (for crust #1 and #2) and 327 Ma, (for crust #3), whereas mantle #1-#5 are the residues produced by extraction of crust #1-#5 (QUE 94201) at 4.525 Ga, and 327 Ma. Note that the shergottites (with the exception of QUE 94201) fall between the calculated mantle and crustal fields on Fig. 7 on a line that has a slope that corresponds to an age of about 1.3 Ga.

The fact that the shergottites fall between the calculated mantle and crustal fields on Fig. 7 is qualitatively consistent with the mixing models proposed by Jones (1989) and Jagoutz (1991), and suggests that the isotopic compositions of the shergottites can be produced by mixing mantle and crustal reservoirs. However, there is significantly more variation observed in the modeled crustal and mantle Sm-Nd isotopic compositions than is required to satisfy a mixing model for the shergottites. The modeled crustal reservoirs have a limited range in $^{147}Sm/^{144}Nd$, but a large range in $^{143}Nd/^{144}Nd$, reflecting the time at which the melt was extracted from the Martian mantle. In contrast, the modeled mantle reservoirs have more variation in $^{147}Sm/^{144}Nd$ than in $^{143}Nd/^{144}Nd$ reflecting the strong fractionation of Sm from Nd during late stage partial melting events. The fact that most of the shergottites fall on a single line indicates that they must be closely related to very similar crustal and mantle reservoirs. Note that QUE 94201 falls significantly off this line suggesting that it is less closely related to the other shergottites and that there may be a sampling bias in the shergottites studied so far. If so, then the ~1.3 Ga whole rock isochron may not be supported by acquisition of additional samples.

Jones (1989) used Nakhla to define the Martian mantle isotopic composition, thereby implying that Shergotty and Zagami are most representative of Martian crust (i.e. they are isotopically the most different from Nakhla). Jagoutz (1991) proposed a similar model, but suggested that there are two distinct mantle reservoirs on Mars. However, in both models the estimated $^{147}Sm/^{144}Nd$ of the mantle was too low to satisfy simple two-component mixing models for the shergottites. Jones (1989) suggested that there was a chemical fractionation of Sm from Nd

immediately preceding shergottite crystallization that depleted the mantle source in Nd relative to Sm. Our analysis of QUE 94201 demonstrates that a mantle source with high Sm/Nd is present on Mars by 327 Ma, and that much of the depletion of Nd relative to Sm occurred near this time. Partial melting of a high $^{147}Sm/^{144}Nd$ QUE 94201-like source (e.g., mantle #4) would produce mantle melts with moderate $^{147}Sm/^{144}Nd$ and high $^{143}Nd/^{144}Nd$ values (Fig. 7). Note that in principal the Sm-Nd systematics of the younger (~180 Ma) shergottites could be satisfied by mixing melts from a single highly-depleted mantle source, such as mantle #4 or mantle #5, with variable combinations of "ancient" (~4.5 Ga) and "young" (~0.3 Ga) crust. Thus, the isotopic variability observed in the shergottites is consistent with assimilation of Martian crustal material by mantle derived melts with high $^{147}Sm/^{144}Nd$ and $^{143}Nd/^{144}Nd$.

Figure 8 is a $^{87}Rb/^{86}Sr$ vs. $^{87}Sr/^{86}Sr$ isochron plot of shergottite and nakhlite whole rock values (recalculated for an average age of the shergottites at 180 Ma), and crustal and mantle reservoirs calculated from the partial melting models. As is the case for the Sm-Nd system, the shergottites fall between mantle and early-formed crustal reservoirs in the Rb-Sr system, again indicative of mixing. In this case, however, the shergottites, nakhlites, and modeled mantle and crustal sources define a whole rock array with a slope that corresponds to an age of about 4.5 Ga. Shih et al. (1982) and Jagoutz (1991) interpreted the SNC meteorite Rb-Sr whole rock isochron as the age of differentiation of the parent body. In our model, the Rb-Sr whole rock isochron more specifically reflects the age at which Rb was completely fractionated from the mantle into crust.

The partial-melting models developed in the previous sections demonstrate that Rb can be effectively partitioned into the early crust after only a few melting events. The Martian mantle can therefore potentially maintain $^{87}Sr/^{86}Sr$ that is near the initial solar system value, whereas crustal rocks (with various $^{87}Rb/^{86}Sr$ values) can evolve to fall along the 4.5 Ga reference line (Fig. 8). Subsequent mixing between mantle and crustal reservoirs yield magmas with Rb-Sr isotopic ratios that also fall near the 4.5 Ga reference line. This scenario is illustrated by QUE 94201. Although QUE 94201 has the lowest initial $^{87}Sr/^{86}Sr$ value (0.701298), it is substantially elevated above the expected value calculated for its source by the partial melting models (0.699097; Table 4). QUE

94201 is therefore likely to have assimilated some crustal material that raised the initial $^{87}Sr/^{86}Sr$ of the melt. The Sm-Nd systematics of the model results presented in Fig. 7 suggests that the crustal component is likely to have both "ancient" (~4.5 Ga) and "young" (~0.3 Ga) components. Nevertheless, QUE 94201 lies on the 4.5 Ga Rb-Sr reference line in Fig. 8 because both "ancient" and "young" crustal sources, as well as the mantle sources, calculated by the partial melting models lie on the 4.5 Ga Rb-Sr reference line.

The leachate data also support our conclusion that the SNC whole rock 4.5 Ga Rb-Sr and 1.3 Ga Sm-Nd isochrons are mixing lines by demonstrating that mixing between crustal and mantle sources within QUE 94201 leachates can produce mixing lines with slopes that are similar to the whole rock isochrons (Figs. 3, 4). Whereas the Rb-Sr whole rock isochron is interpreted to reflect that time when Rb was partitioned into the crust, there is less significance to the 1.3 Ga Sm-Nd whole rock isochron age. This stems from the inability of geologic processes to completely fractionate Sm from Nd. The fact that the Sm-Nd whole rock isochron is younger than the Rb-Sr isochron reflects the greater proficiency with which differentiation processes have fractionated Rb from Sr compared to Sm from Nd. As a result, the crust is likely to have virtually all of the Rb and radiogenic Sr, but subequal amounts of Sm and Nd compared to the mantle. There is thus a greater potential for the Rb-Sr systematics of mantle melts to be affected by a given amount of assimilation than the Sm-Nd systematics, and hence there is a decoupling of Rb-Sr and Sm-Nd systems in the SNC meteorites.

The absence of Rb in the Martian mantle since the time of the first differentiation events, and subsequent decoupling of the Rb-Sr and the Sm-Nd isotopic systems, suggests that crustal recycling processes have not occurred on Mars. Re-introduction of large ion lithophile elements (LILE), such as Rb, into the Martian mantle via subduction-like processes would result in higher and more variable $^{87}Sr/^{86}Sr$ in mantle-derived melts, making the Rb-Sr isotopic systematics, and in particular the 4.5 Ga Rb-Sr whole rock isochron, difficult to explain. The presence of large ε_{Nd}^{142} anomalies in young (327 Ma and 1.3 Ga) melts further argues against crustal recycling processes that could easily obscure ^{142}Nd enrichments by dilution with "crustal" Nd that has a

normal abundance of ^{142}Nd. The apparent absence of crustal recycling and the relative isolation of the Martian mantle from the Martian crust is one of the most significant geologic differences between Mars and the Earth.

CONCLUSIONS

Isotopic analyses of minerals, leachates, and whole rock fractions from the basaltic shergottite QUE 94201 yield Rb-Sr and Sm-Nd crystallization ages of 327±12 and 327±19, respectively. The presence of leachable secondary alteration products in several of the mineral fractions variably affects their Rb-Sr and Sm-Nd systematics, and results in Rb-Sr and Sm-Nd internal isochrons that are defined by different fractions. Initial $^{87}Sr/^{86}Sr$ and ε_{Nd}^{143} values of 0.701298 and +47.6, and a whole rock ε_{Nd}^{142} value of +0.92 indicate that QUE 94201 was derived from a source that was strongly depleted in $^{87}Rb/^{86}Sr$ and enriched in $^{147}Sm/^{144}Nd$ early in its history. Partial melting models demonstrate that the Sm-Nd isotopic composition of QUE 94201 can be produced from a chondritic source by five episodes of melting (two occurring at 4.525 Ga and three occurring at 327 Ma). The Nd isotopic systematics of QUE 94201 are not consistent with fewer than five melting events, or significant melting between 4.500 Ga and 327 Ma, and the initial depletion of the QUE 94201 source later than 4.500 to 4.525 (depending if garnet is assumed in the source). Numerous melting events effectively partition virtually all Rb into the Martian crust near 4.5 Ga. Subsequent mixing of crustal and mantle reservoirs produces the 4.5 Ga Rb-Sr whole rock isochron observed in the SNC meteorites. If this scenario is correct, then the 1.3 Ga whole rock isochron defined by all the shergottites (except QUE 94201) also represents a mixing line. The difference in age between the Rb-Sr and Sm-Nd whole rock isochrons is a manifestation of a decoupling of the two isotopic systems on Mars. This decoupling ultimately results from the absence of large scale recycling of crust back into the Martian mantle and may be one of the most significant geologic differences between Mars and the Earth.

REFERENCES

Borg L. E., Nyquist L. E., Wiesmann H. and Shih C.-Y. (1996) Rubidium-Strontium age and initial $^{87}Sr/^{86}Sr$ of basaltic shergottite QUE 94201 (abstr). *Meteoritics* **31,** 18.

Dreibus G. and Wänke H. (1985) Mars, a volatile-rich planet. *Meteoritics* **20,** 367-381.

Gleason J. D., Kring D. A. and Boynton W. V. (1996) The role of garnet in Martian evolution: Further evidence from Shergottite rare earth patterns (abstr). Lunar Planet. Sci. Conf. XXVII, 425-426.

Harper C. L., Nyquist L. E., Bansal B., Wiesmann H. and Shih C. -Y. (1995) Rapid accretion and early differentiation of Mars indicated by $^{142}Nd/^{144}Nd$ in SNC meteorites. *Science* **267,** 213-217.

Harvey, R. P., McCoy T. J. and Leshin L. A. (1996) Shergottite QUE 94201: Textural, mineral compositions, and comparison with other basaltic shergottites (abstr). Lunar Planet. Sci. Conf. XXVII, 497-498.

Jagoutz, E. (1989) Sr and Nd isotopic systematics in ALHA 77005: Age of shock metamorphism in shergottites and magmatic differentiation on Mars. *Geochim. Cosmochim. Acta* **53,** 2429-2441.

Jagoutz E. (1991) Chronology of SNC meteorites. *Space Sci. Rev.* **56,** 13-22.

Jagoutz E. (1996) Nd isotopic systematics of Chassigny (abstr). Lunar Planet. Sci. Conf. XXVII, 597-598.

Jagoutz E. and Wänke H. (1986) Sr and Nd isotopic systematics of Shergotty meteorite. *Geochim. Cosmochim. Acta* **50,** 939-953.

Jagoutz E., Palme H., Badderhausen H., Blum R., Cendales M., Dreibus G., Spettel B., Lorenz V. and Wänke H. (1979) The abundances of major, minor, and trace elements in the earth's mantle as derived from primitive ultramafic nodules. *Proc. Lunar Planet Sci Conf.* **10,** 2031-2050.

Johnson M. C., Rutherford M. J. and Hess, P. C. (1991) Chassigny petrogenesis: Melt compositions, intensive parameters, and water contents of Martian (?) magmas. *Geochim. Cosmochim. Acta* **55,** 349-366.

Jones J. H. (1986) A discussion of isotopic systematics and mineral zoning in the shergottites: Evidence for a 180 m.y. igneous crystallization age. *Geochim. Cosmochim. Acta* **50,** 969-977.

Jones J. H. (1989) Isotopic relationships among Shergottites, the Nakhlites and Chassigny. *Proc. Lunar Planet Sci Conf.* **19,** 465-475.

Jones J. H. (1995) Experimental trace element partitioning. in Rock Physics and Phase Relations . A handbook of physical constraints, AGU reference Shelf 3, pp. 73-104.

Kay R. W. (1978) Aleutian magnesian andesites: Melts from subducted Pacific ocean crust, *J. Volcanol. Geotherm. Res.* **4,** 117-132.

Kring D. A., Gleason J. D., Hill D. H., Jull A. J. T. and Boynton, W. V. (1996) QUE 94201, a new Martian meteorite that may represent a bulk melt rather than a cumulate fraction (abstr) Lunar Planet. Sci. Conf. XXVII, 705-706.

Longhi J. (1991) Complex magmatic processes on Mars: Inferences from SNC meteorites. *Proc. Lunar Planet Sci Conf.* **21,** 465-475.

Longhi J. and Pan V. (1988) A reconnaissance study of phase boundaries in low-alkali basaltic liquids. *J. Petrol.* **29,** 115-148.

Longhi J. and Pan V. (1989) The parent magmas of the SNC meteorites. *Proc. Lunar Planet Sci Conf.* **19,** 451-464.

Longhi J., Knittle E., Holloway J. R. and Wänke H. (1992) The bulk composition, mineralogy and internal structure of Mars. In Mars, Kieffer H., Jakosky B., Snyder C. and Mathews M. S. (eds). Univ. Ariz. Press, Tucson and London pp. 184-208.

Lugmair G. W. and Galer S. J. G. (1992) Age and isotopic relationships among angrites Lewis Cliff 86010 and Angra dos Reis. *Geochim. Cosmochim. Acta* **56,** 1673-1694.

McKay G. A. (1986) Crystal/liquid partitioning of REE in basaltic systems: Extreme fractionation of REE in olivine. *Geochim. Cosmochim. Acta* **50,** 69-79.

McKay G. A., Wagstaff J., Yang S. -R. (1986) Clinopyroxene REE distribution coefficients for shergottites: The REE content of the Shergotty melt *Geochim. Cosmochim. Acta* **50,** 927-937.

McKay G. A., Yang S. -R. and Wagstaff J. (1996) Complex zoned pyroxenes in shergottite QUE 94201: Evidence for a two-stage crystallization history. (abstr). Lunar Planet. Sci. Conf. XXVII, 851-852.

McKenzie D. and O'Nions R. K. (1991) Partial melt distributions from inversion of rare earth element concentrations. *J. Petrol.* **32,** 1021-1091.

McSween H. Y., JR. (1994) What we have learned about Mars from SNC meteorites. *Meteoritics* **29,** 757-779.

McSween H. Y., JR. and Eisenhour D. D. (1996) QUE 94201, a noncumulate shergottite? (abstr) Lunar Planet. Sci. Conf. XXVII, 53-54.

McSween H. Y., JR., Eisenhour D. D., Taylor L. A., Wadwa M. and Crozaz G. (1996) QUE 94201 Shergottite: Crystallization of a Martian basaltic magma. *Geochim. Cosmochim. Acta* **60,** 4563-4569.

Mittlefehldt D. W. and Lindstrom M. M. (1996) Martian meteorites QUE 94201, an unusual basalt, Governador Valadares, a typical clinopyroxenite: Geochemistry. (abstr) Lunar Planet. Sci. Conf. XXVII, 887-888.

Mikouchi T., Miyamoto M. and McKay G. A. (1996) Mineralogy and petrology of new Antarctic shergottite QUE 94201: A coarse-grained basalt with unusual pyroxene zoning (abstr) Lunar Planet. Sci. Conf. XXVII, 879-880.

Misawa, K., Tatsumoto, M., Dalrymple, G. B., and Yanai, K. (1993) An extremely low U/Pb source in the Moon: U-Th-Pb, Sm-Nd. Rb-Sr, and $^{40}Ar/^{39}Ar$ isotopic systematics and age of lunar meteorite Asuka 881757. *Geochim. Cosmochim. Acta* **57,** 4687-4702.

Nakamura N., Unruh D. M., Tatsumoto M. and Hutchison R. (1982) Origin and evolution of the Nakhla meteorite inferred from Sm-Nd and U-Pb systematics and REE, Ba, Sr, Rb, and K abundances. *Geochim. Cosmochim. Acta* **46,** 1555-1573.

Nyquist L. E., Wooden J. L., Bansal B. M., Wiesmann H., McKay G. and Bogard D. D. (1979) Rb-Sr age of the Shergotty achondrite and implications for metamorphic resetting of isochron ages. *Geochim. Cosmochim. Acta* **43,** 1057-1074.

Nyquist L. E., Bansal B., Wiesmann H., Shih C. -Y. (1995a) "Martians" young and old: Zagami and ALH 84001. (abstr) Lunar Planet. Sci. Conf. XXVI, 1065-1066.

Nyquist L. E., Wiesmann H., Bansal B., Shih C. -Y., Keith J. E. and Harper C. L. (1995b) ^{146}Sm-^{142}Nd formation interval for the lunar mantle. *Geochim. Cosmochim. Acta* **59,** 2817-2837.

Shih C. -Y., Nyquist L. E., Bogard D. D., McKay G. A., Wooden J. L., Bansal B. M. and Wiesmann H. (1982) Chronology and petrogenesis of young achondrites, Shergotty, Zagami, and ALHA 77005: Late magmatism on a geologically active planet *Geochim. Cosmochim. Acta* **46,** 2323-2344.

Shih C. -Y., Nyquist L. E. and Wiesmann H. (1996) Sm-Nd systematics of nakhlite Governador Valadares. (abstr) Lunar Planet. Sci. Conf. XXVII, 1197-1198.

Snyder, G. A., Lee, D.-C., Taylor, L. A., Halliday, A. N., and Jerde, E. A. (1994) Evolution of the upper mantle of the Earth's Moon: Neodymium and strontium isotopic constraints from high Ti-mare basalts *Geochim. Cosmochim. Acta* **58,** 4795-4808.

Stolper E. M. and McSween H. Y., JR. (1979) Petrology and origin of the shergottite meteorites. *Geochim. Cosmochim. Acta* **43,** 1475-1498.

Sun S. S. and McDonough, W. F. (1989) Chemical and isotopic systematics of oceanic basalts: Implications for mantle composition and processes, In: Saunders, A. D. & Norry, M. J. (eds.) Magmatism in the Ocean Basins. London: Blackwell Scientific Publications, published for the Geological Society, pp. 313-345.

Treiman A. H. (1986) The parental magma of the Nakhla achondrite: Ultrabasic volcanism on the shergottite parent body. *Geochim. Cosmochim. Acta* **50,** 1061-1070.

Treiman A. H., Drake M. J., Janssens M. -J, Wolf R. and Ebihara M. (1986) Core formation in the Earth and Shergottite parent body (SPB): Chemical evidence from basalts. *Geochim. Cosmochim. Acta* **50,** 1071-1091.

Wadwa M. and Crozaz G. (1996) QUE 94201: A new and different shergottite. (abstr) Lunar Planet. Sci. Conf. XXVII, 1365-1366.

Warren P. H., Kallemeyn G. W., Arai T. and Kaneda K. (1996) Compositional-petrologic investigation of eucrites and the QUE94201 shergottite. (abstr) Symposium on Antarctic Meteorites XXI, 195-197.

Wänke H. and Dreibus G. (1988) Chemical composition and accretional history of terrestrial planets. *Phil. Trans. Roy. Soc. London* **A235,** 545-557.

Wentworth S. J. and Gooding J. L. (1996) Water-based alteration of the Martian meteorite, QUE 94201, by sulfate-dominated solutions. (abstr) Lunar Planet. Sci. Conf. XXVII, 1421-1422.

Williamson J. H. (1968) Least-squares fitting of a straight line. *Can. J. Phys.* **46,** 1845-1847.

Wooden J. L., Nyquist L. E., Bogard D. D., Bansal B. M., Wiesmann H. and Shih C. -Y (1979) Radiometric ages for the achondrites Chevony Kut, Governador Valadares, and Allan Hills 77005. (abstr) Lunar Planet. Sci. Conf. X, 379-1381.

Wooden J. L., Shih C. -Y, Nyquist L. E., Bansal B. M., Wiesmann H. and McKay G. (1982) Rb-Sr and Sm-Nd isotopic constraints on the origin of EETA 79001: A second Antarctic shergottite. (abstr) Lunar Planet. Sci. Conf. XIII, 879-880.

York D. (1966) Least squares fitting of a straight line. *Can. J. Phys.* **44,** 1079-1086.

TABLE 1. Rb-Sr analytical results for QUE 94201

Fraction	Wt. (mg)	Rb (ppm)	Sr (ppm)	$^{87}Rb/^{86}Sr$[a]	$^{87}Sr/^{86}Sr$[b]
WR-1	15.25	0.518	41.3	0.0363±2	0.701532±14
WR 2	52.50	0.691	49.8	0.0402±2	0.701481±13
WR-L[c]	4.80	0.635	135.9	0.0135±1	0.701626±15
Plag-1R	3.00	0.268	108.0	0.00719±7	0.701335±15
Plag-2	15.75	0.314	109.6	0.00829±4	0.701327±15
Plag-3L[c]	3.71	0.0057	1.76	0.00939±33	0.701285±15
Fe-Pyx-R	45.03	0.174	3.51	0.143±1	0.701942±18
Fe-Pyx-L	---	---	---	0.0420±51	0.702364±14
Mg-Pyx-R	15.95	0.0892	4.37	0.0591±3	0.701581±15
Mg-Pyx-L	---	---	---	0.0177±4	0.701719±15
Pyx-R	2.75	0.224	4.51	0.144±2	0.701970±20
Glass-1R	3.30	0.793	5.75	0.399±2	0.703019±39
Glass-2	29.40	1.83	27.2	0.195±44	0.702272±16
NBS-987 (N=21)					0.710247±22[d]

a Error limits apply to the last digits and include minimum uncertainty of 0.5% plus 50% of the blank correction for Rb and Sr added quadratically.

b Normalized to $^{86}Sr/^{88}Sr = 0.1194$. Uncertainties refer to last digits and are $2\sigma_m$ calculated from measured isotopic ratios.
$\sigma_m = [\Sigma(m_i-\mu)^2/(n(n-1))]^{1/2}$ for n ratio measurements m_i with mean value μ.
$\sigma_p = [\Sigma(M_i-\pi)^2/(N-1))]^{1/2}$ for N measurements M_i with mean value π.

c Weight calculated by difference between unleached fraction and residue.

d Uncertainties refer to last digits and are $2\sigma_p$. Isochrons are calculated using either $2\sigma_p$ (from standard runs) or $2\sigma_m$ (from measured isotopic ratios), whichever is larger.

TABLE 2. Sm-Nd analytical results for QUE 94201

Fraction	Wt. (mg)	Sm (ppm)	Nd (ppm)	Nd (ng)	$^{147}Sm/^{144}Nd$[a]	$^{142}Nd/^{144}Nd$[b]	$\varepsilon_{Nd}{}^{142}$[c]	$^{143}Nd/^{144}Nd$[b]
run as NdO^+								
WR-1	15.25	1.233	1.482	23	0.5031±5	1.138452±16	1.07±0.78	0.514898±6
WR-L[d]	4.80	27.25	34.09	164	0.4834±5	1.138436±20	0.93±0.78	0.514847±9
Plag-1R	3.00	0.250	0.273	0.8	0.5542±89	---	---	0.514158±170
Plag-2	15.75	0.0919	0.407	6.4	0.1364±4	---	---	0.511439±10
Plag-3L[d]	3.71	0.125	0.541	2.0	0.1349±14	---	---	0.512336±91
Fe-Pyx-R	45.03	0.165	0.113	5.1	0.8834±22	---	---	0.515766±12
Fe-Pyx-L	---	---	---	---	0.4707±6	---	---	0.514710±15
Mg-Pyx-R	15.95	0.306	0.215	3.4	0.8582±32	---	---	0.515680±12
Mg-Pyx-L	---	---	---	---	0.4775±6	---	---	0.514742±45
Pyx-R	2.75	0.196	0.139	0.4	0.849±28	---	---	0.515157±80
Glass-1R	3.30	0.0410	0.134	0.4	0.183±71	---	---	0.511872±120
AMES Nd Std (N = 12)						1.138330±89[e]		0.511103±46[e]
run as Nd^+								
WR-L[d]	4.80	27.25	34.09	164	0.4834±5	1.138360±17	0.80±0.26	0.514835±6
Glass-2	29.40	1.696	2.091	62	0.4905±25	1.138382±70	0.99±0.62	0.514834±35
WR-2[f]	52.50	---	---	---	---	1.138374±14	0.92±0.11	0.514824±6
AMES Nd Std (N = 37)						1.138269±27[e]		0.511103±14[e]

0.1-1V ^{144}Nd beam intensities for NdO^+ runs of unknowns and standards, and 0.3-3V ^{144}Nd beam intensities for Nd^+ runs of unknowns and standards.

a Error limits apply to the last digits and include minimum uncertainty of 0.1% plus 50% of the blank correction for Sm and Nd added quadratically.

b Normalized to $^{146}Nd/^{144}Nd = 0.72414$. Uncertainties refer to last digits and are $2\sigma_m$ calculated from measured isotopic ratios.

$\sigma_m = [\Sigma(m_i-\mu)^2/(n(n-1))]^{1/2}$ for n ratio measurements m_i with mean value μ.

c $\varepsilon_{Nd}{}^{142}$ anomaly determined from unspiked whole rock run (WR-2). $\varepsilon_{Nd}{}^{142}$ calculated for mineral fractions to show consistent with WR-2 value.

d Weight calculated by difference between unleached fraction and residue.

e Uncertainties refer to last digits and are $2\sigma_p$. Isochrons are calculated using either $2\sigma_p$ (from standard runs) or $2\sigma_m$ (from measured isotopic ratios) whichever is larger.

$\sigma_p = [\Sigma(M_i-\pi)^2/(N-1))]^{1/2}$ for N measurements M_i with mean value π.

f Unspiked sample run for ^{142}Nd. Average of six runs on sample filament.

TABLE 3. Partition coefficients used in models

	Sm	Nd	Rb	Sr
Ol	0.0006[a]	0.00007[a]	0.0002[c]	0.0002[c]
Opx	0.019[b]	0.031[b]	0.0006[c]	0.007[c]
Cpx	0.17[b]	0.104[b]	0.0019[d]	0.12[e]
Grt	0.29[c]	0.068[c]	0.001[d]	0.04[d]

a McKay (1986).
b McKay et al. (1986).
c McKenzie and O'Nions (1991).
d Kay (1978).
e Jones (1995).

TABLE 4 Results of time-integrated partial melting models

	$t_{melting}$ (Ga)[a]	Nd (ppm)	Sm (ppm)	$^{147}Sm/^{144}Nd$	ε_{Nd}^{143} (present)	ε_{Nd}^{142}	Sr (ppm)	Rb (ppm)	$^{87}Rb/^{86}Sr$	$^{87}Sr/^{86}Sr$ (present)
Initial (2xCI)[b]	4.558	0.905	0.294	0.1967	0	0	14.52	0.821	0.160	0.698970
1st melt[c]	4.525	26.8	4.29	0.097	-58.6		477	118	0.703	0.743335
1st residua		0.664	0.257	0.234	21.9	0.41	10.2	0.081	0.022	0.700501
2nd melt	4.525	19.7	3.77	0.116	-47.4		335	7.92	0.067	0.703409
2nd residua		0.482	0.233	0.2801	49.0	0.92	7.10	0.005	0.0021	0.699184
3rd melt	0.327	7.96	2.41	0.183	44.7		124	0.14	0.0032	0.699188
3rd residua		0.187	0.137	0.444	55.6	0.92	2.48	$9.3E^{-5}$	$1.1E^{-4}$	0.699174
4th melt	0.327	3.14	1.38	0.266	48.1		44.3	$2.4E^{-3}$	$1.5E^{-4}$	0.699174
4th residua		0.079	0.110	0.839	68.8	0.92	0.83	$1.7E^{-6}$	$5.9E^{-6}$	0.699173
5th melt	0.327	1.20	1.00	0.504	58.1		15.2	$4.5E^{-5}$	$8.4E^{-6}$	0.699173
5th residua		0.025	0.052	1.24	88.9	0.92	0.27	$2.9E^{-8}$	$3.1E^{-7}$	0.699173
QUE 94201[d]	0.327	1.48	1.23	0.503	58.6	0.92	49.8	0.691	0.0402	0.701298

a Time at which sources were produced.
b Initial composition estimated from C1 chondrites (see text).
c Modeled melts represent crustal sources, and modeled residua represent mantle sources.
d Sm and Nd from WR-1, and Rb and Sr from WR-2.

Figure Captions

Figure 1. Chondrite-normalized spider diagram of shergottites, nakhlites and QUE 94201. Average values for individual meteorites summarized in Treiman et al. (1986) are used to define the field for the shergottites (ALHA 77005, EETA 79001 A and B, Shergotty, and Zagami) and the field for the nakhlites (Nakhla and Lafayette). Normalization to CI chondrite values of Sun and McDonough (1989). Data for QUE 94201 is average of values from Warren et al. (1996), Mittlefehldt and Lindstrom (1996), and this study. Note that the Nakhlites have high LREE and low HREE relative to the shergottites. Also note that QUE 94201 is strongly depleted in the most incompatible elements (e.g., Rb, Ta, K, and LREE) and relatively enriched in HREE.

Figure 2. Flow diagram illustrating mineral separation procedure. Shaded fractions were analyzed for Rb-Sr and Sm-Nd. All fractions were hand picked and were very pure (>99.5%). Composite grains of primarily glass and pyroxene removed by hand-picking the Pyx-R (Glass-1R) and Fe-Pyx and Mg-Pyx (Glass-2) were also analyzed.

Figure 3. Rb-Sr isochron plot of mineral, leachate, and whole rock fractions from QUE 94201 calculated using the program of Williamson (1968). A crystallization age of 327±12 Ma and an initial $^{87}Sr/^{86}Sr$ of 0.701298±14 is defined by Plag-1R, Plag-2, WR-2, Mg-Pyx-R, Fe-Pyx-R, and Pyx-R (solid circles) using $\lambda(^{87}Rb) = 0.01402\ (Ga)^{-1}$. The MSWD for this isochron is 1.11. An age of 327±28 Ma is calculated using the same data points and the program of York (1966). Open circles are analyzed fractions not used to define the isochron. The Rb-Sr age is based on analyses of mineral residues and one whole rock, and is therefore unlikely to be effected by post-crystallization addition of secondary sulfate and phosphate phases observed in QUE 94201 by Harvey et al. (1996) and Wentworth and Gooding (1996). Leachates do not lie on the 327 Ma isochron because they contain a secondary crustal component, and have isotopic compositions that are likely to reflect mixtures of primary mantle-like and secondary crustal components. Note that

the leachates lie near a line with a slope corresponding to an age of 4.2 Ga. Inset shows analytical uncertainty of individual points used to define the isochron. ε_{Sr} represents deviation of an individual point from the isochron calculated by:

$\varepsilon_{Sr} = [(^{87}Sr/^{86}Sr)^{measured}/(^{87}Sr/^{86}Sr)^{isochron}-1]*10000.$

Figure 4. Sm-Nd isochron plot of mineral, leachate, and whole rock fractions from QUE 94201 calculated using the program of Williamson (1968). A crystallization age of 327±19 Ma and an initial ε_{Nd}^{143} of +47.4±3.5 is defined by NdO^- runs of Mg-Pyx-R, Fe-Pyx-R, WR-1, and WR-L (solid circles) using $\lambda(^{147}Sm) = 0.00654$ $(Ga)^{-1}$. The MSWD for this isochron is 1.14. An age of 327±35 Ma is calculated using the same data points and the program of York (1966). Open circles are analyzed fractions not used to define the isochron. These fractions contain less than 0.8 ng of Nd, are leachates, or are unleached mineral separates (see text) and are therefore susceptible to blank corrections and/or secondary alteration observed in the rock. The 327±19 age is concordant with the Rb-Sr age, although it is defined by different fractions within the meteorite. The leachates fall off the 327 Ma isochron, probably as a result of secondary addition of crustal components, along a line with a slope corresponding to an age of about 1.1 Ga. Note that the plagioclase fractions have variable Sm-Nd systematics, and that unleached Plag-2 and the Plag-3L leachate have very low $^{147}Sm/^{144}Nd$ and $^{143}Nd/^{144}Nd$, consistent with presence of a secondary LREE-enriched crustal component in these fractions. Inset shows analytical uncertainty of individual points used to define the isochron. ε_{Nd} represents deviation of an individual point from the isochron calculated by:

$\varepsilon_{Nd} = [(^{143}Nd/^{144}Nd)^{measured}/(^{143}Nd/^{144}Nd)^{isochron}-1]*10000.$

Figure 5. Chondrite-normalized plot of Nd and Sm concentrations determined by isotope dilution analyses on mineral fractions and in situ ion microprobe analyses by Wadwa and Crozaz (1996) and McSween et al. (1996). Normalization to values of Sun and McDonough (1989).

WR-L and whitlockite have similar Nd and Sm concentrations suggesting the leachate is dominated by the igneous whitlockite component. The Mg-Pyx-R and Fe-Pyx-R have concentrations that are similar to the range of ion microprobe analyses, which is consistent with the observations that these fractions lie on the isochron. The Plag-1R, Plag-2, and Plag-3L fractions have lower Sm/Nd ratios and higher REE concentrations than the maskelynite analyzed by ion microprobe, suggesting that these fractions are contaminated with a secondary LREE-enriched crustal component. Note that of all the plagioclase fractions Plag-1R has a Sm/Nd ratio that is closest to the value determined by ion microprobe and plots closest to the isochron in Fig. 4.

Figure 6. T-ε_{Nd}^{143} diagram illustrating the results of partial melting models. Multi-stage melting models reproduce the Nd, Sm concentrations, $^{147}Sm/^{144}Nd$, $^{143}Nd/^{144}Nd$ and $^{142}Nd/^{144}Nd$ measured in QUE 94201 starting with a source with 2xC1 abundances of Sm and Nd. Five melting events are required to produce a strongly LREE depleted melt such as QUE 94201 from a chondritic source. Source mineralogy is Ol:Opx:Cpx:Gar = 60:17:10:13 and is melted in the proportions Ol:Opx:Cpx:Gar = 31:19:27:23. The timing of initial melting events is constrained by ε_{Nd}^{142} to be 33 Ma after solar condensation at 4.525 Ga producing crust #1 and mantle #1 (not shown). This is followed by a second melting event at the same time which produces crust #2 and mantle #2 with $^{147}Sm/^{144}Nd$ of 0.281. Later melting events must be roughly contemporaneous with QUE 94201 melt production at 327 Ma in order to produce the observed initial ε_{Nd}^{143}. The timing and extent of the two early melting events are, therefore, fixed by the $^{143}Nd/^{144}Nd$ and $^{142}Nd/^{144}Nd$ of QUE 94201, since melting occurring at 327 Ma will not affect its isotopic systematics. Although the ^{142}Nd anomaly observed in QUE 94201 can be produced by large degrees of melting after 4.525 Ga (i.e. from a source with $^{147}Sm/^{144}Nd > 0.281$), the $^{143}Nd/^{144}Nd$ of the modeled melt will be too high. Likewise smaller degrees of melting must occur prior to 4.525 Ga to produce the observed ^{142}Nd anomaly, but yield melts with $^{143}Nd/^{144}Nd$ that is too low. Two melting events occurring at 327 Ma produce crust #3, crust #4,

mantle #3, and mantle #4. The final melting event produces the QUE 94201 melt (crust #5) and a residua (mantle #5). See table 4 for detailed model results.

Figure 7. Sm-Nd plot of shergottite whole rocks, and modeled crustal and mantle reservoirs calculated at 180 Ma (the crystallization age of most shergottites). Ages in parentheses represent the time that the mantle and crustal sources were produced by melting events. Shergottite data from Nyquist et al. (1979), Shih et al. (1982) and Wooden et al. (1982). Note that the shergottites, with the exception of QUE 94201, fall on a line with a slope corresponding to an age of 1.3 Ga (t ≈ 1.1 Ga at 180 Ma) that runs between modeled mantle and crustal sources. Partial melting of sources that have strongly time-integrated depletions in incompatible elements generates melts with high $^{143}Nd/^{144}Nd$, but $^{147}Sm/^{144}Nd$ that is lower than the initial source. Mixing between such mantle melts and crust may produce the isotopic systematics of the shergottites. Note that QUE 94201 does not fall on the mixing line defined by the other shergottites, suggesting that it is more distantly related. The presence of a large ε_{Nd}^{142} anomaly in QUE 94201 (and the absence of large anomalies in the other shergottites) suggest that it is probably derived from a different mantle source.

Figure 8. Rb-Sr plot of shergottite and nakhlite whole rocks, and modeled crustal and mantle reservoirs calculated at 180 Ma. Ages in parentheses represent the time that the mantle and crustal reservoirs were produced by melting events. Shergottite and nakhlite data from Shih et al. (1982), Wooden et al. (1979, 1982), Nakamura (1982), Jagoutz and Wänke (1986), and Shih et al. (1996). The shergottites and the nakhlites fall along a line with a slope corresponding to an age of ~4.5 Ga (t ≈ 4.3 Ga at 180 Ma) and between modeled mantle and crustal reservoirs. Crust #1 has high $^{87}Rb/^{86}Sr$ and $^{87}Sr/^{86}Sr$ and lies on the 4.5 Ga reference line because it was extracted from the mantle at 4.525 Ga. The modeled mantle has very low $^{87}Sr/^{86}Sr$ as a result of efficient extraction of Rb by early differentiation processes. The shergottites and nakhlites have measured $^{87}Rb/^{86}Sr$ and $^{87}Sr/^{86}Sr$ values that are higher than modeled mantle compositions, suggesting that

they are mixtures of old crustal, with high $^{87}Rb/^{86}Sr$ and $^{87}Sr/^{86}Sr$, and young mantle sources, with low $^{87}Rb/^{86}Sr$ and $^{87}Sr/^{86}Sr$. Mixing between mantle and crustal sources produces a series of melts that will lie on the 4.5 Ga reference line.

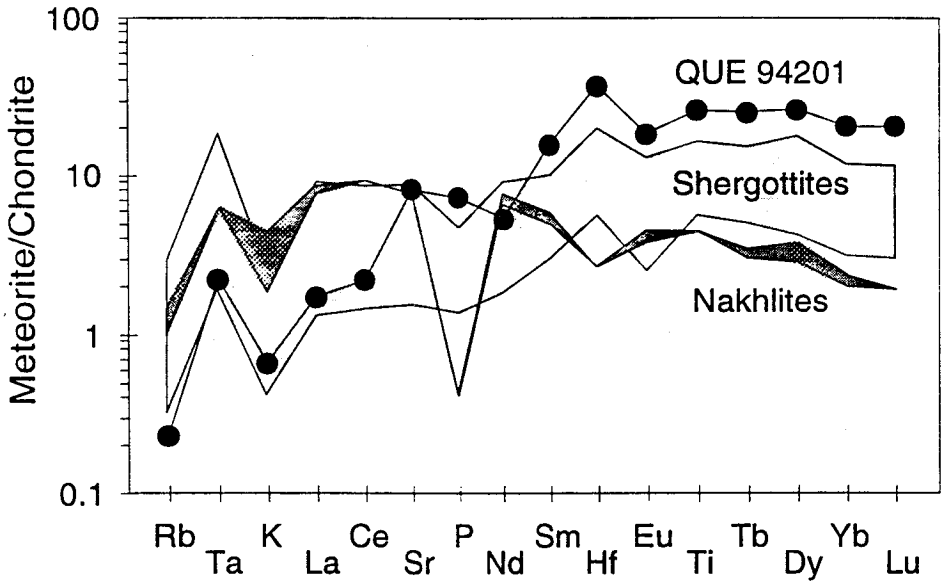
100
10
1
0.1
Meteorite/Chondrite
QUE 94201
Shergottites
Nakhlites
Rb
Ta
K
La
Ce
Sr
P
Nd
Sm
Hf
Eu
Ti
Tb
Dy
Yb
Lu

Figure 1.

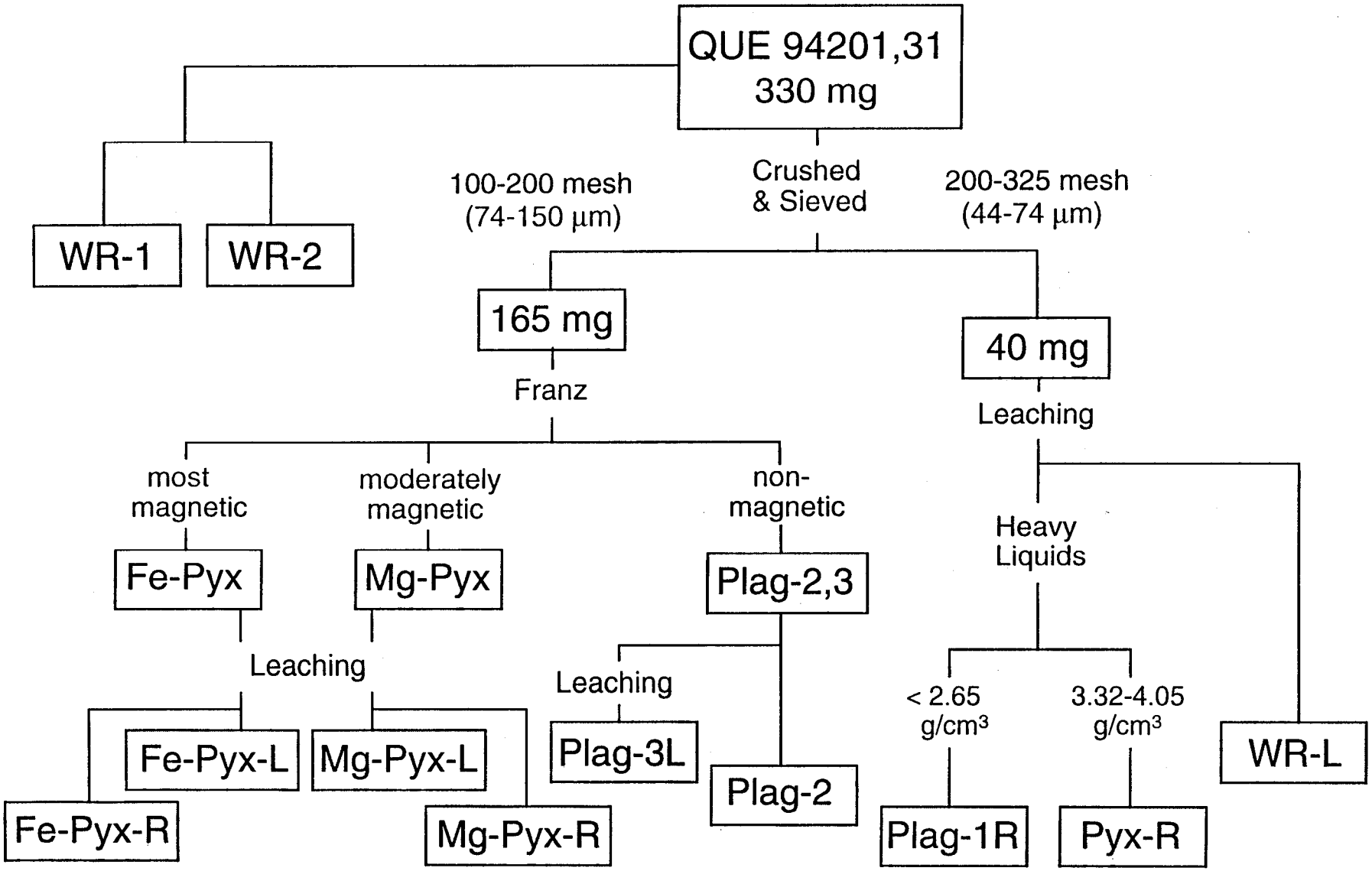
QUE 94201,31
330 mg
WR-1
WR-2
Crushed & Sieved
100-200 mesh (74-150 μm)
200-325 mesh (44-74 μm)
165 mg
40 mg
Franz
Leaching
most magnetic
moderately magnetic
non-magnetic
Heavy Liquids
Fe-Pyx
Mg-Pyx
Plag-2,3
Leaching
Leaching
< 2.65 g/cm3
3.32-4.05 g/cm3
WR-L
Fe-Pyx-L
Mg-Pyx-L
Plag-3L
Plag-2
Fe-Pyx-R
Mg-Pyx-R
Plag-1R
Pyx-R

Figure 2.

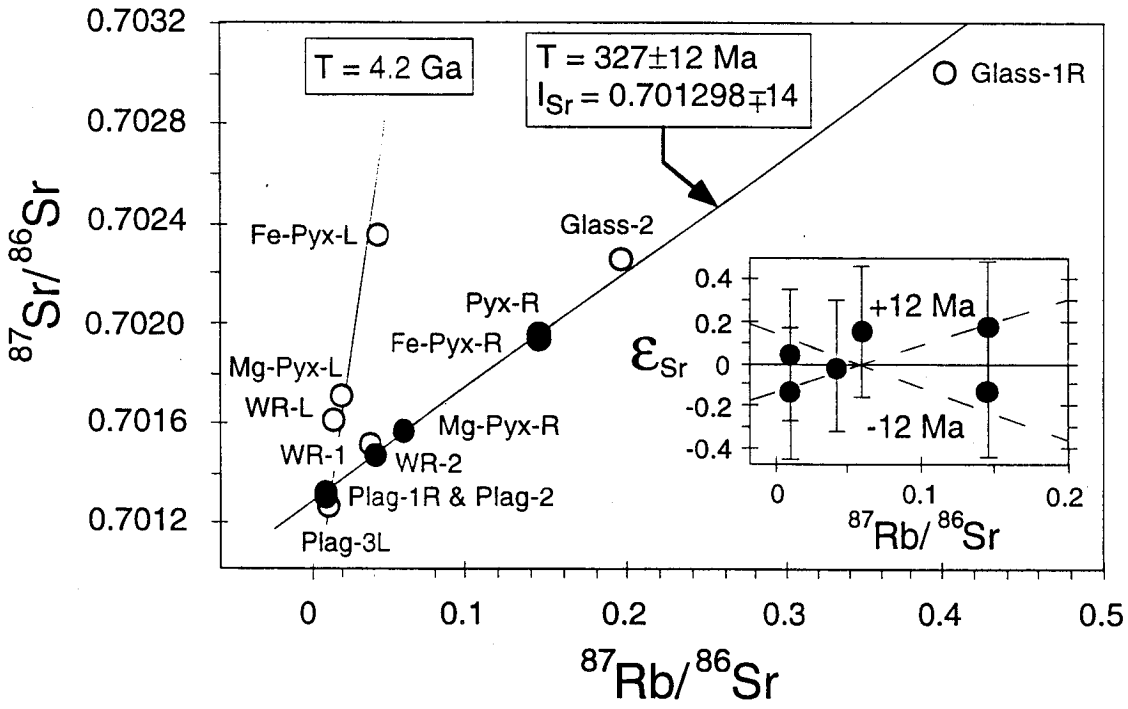
T = 4.2 Ga
T = 327±12 Ma
I_{Sr} = 0.701298∓14
Glass-1R
Glass-2
Fe-Pyx-L
Pyx-R
Fe-Pyx-R
Mg-Pyx-L
WR-L
Mg-Pyx-R
WR-1
WR-2
Plag-1R & Plag-2
Plag-3L
ε_{Sr}
+12 Ma
-12 Ma
$^{87}Rb/^{86}Sr$
$^{87}Sr/^{86}Sr$
0.7032
0.7028
0.7024
0.7020
0.7016
0.7012
0
0.1
0.2
0.3
0.4
0.5
0.4
0.2
0
-0.2
-0.4

Figure 3.

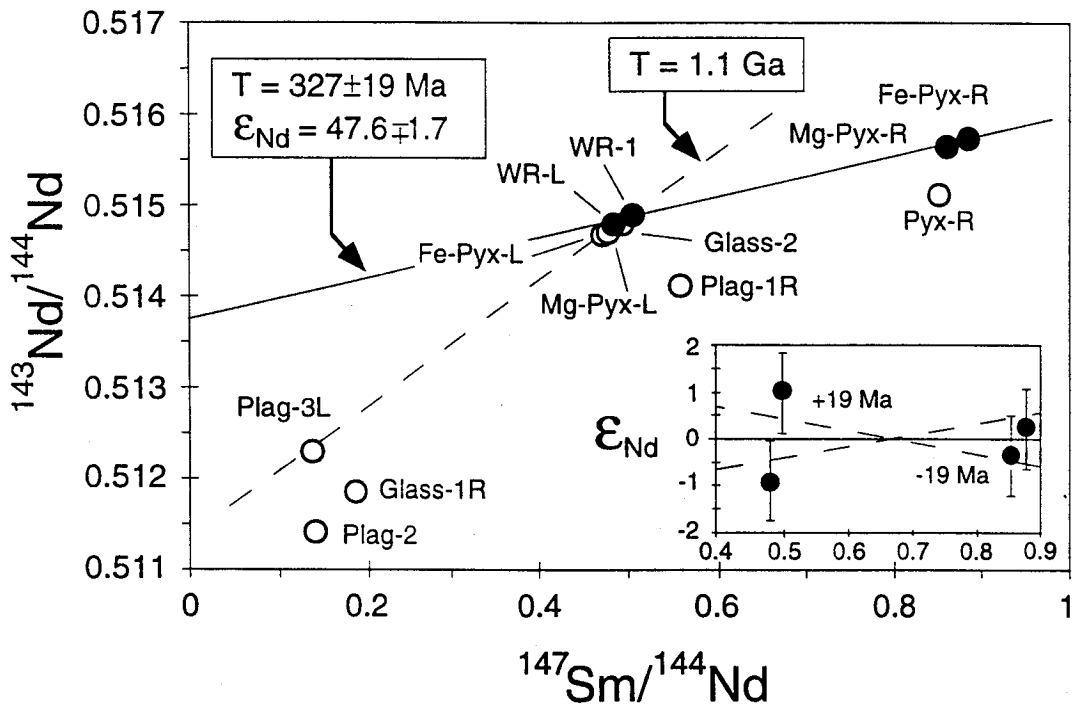
T = 327±19 Ma
εNd = 47.6∓1.7
T = 1.1 Ga
Fe-Pyx-R
Mg-Pyx-R
WR-1
WR-L
Pyx-R
Glass-2
Fe-Pyx-L
Plag-1R
Mg-Pyx-L
Plag-3L
Glass-1R
Plag-2
εNd
+19 Ma
-19 Ma
143Nd/144Nd
147Sm/144Nd

Figure 4.

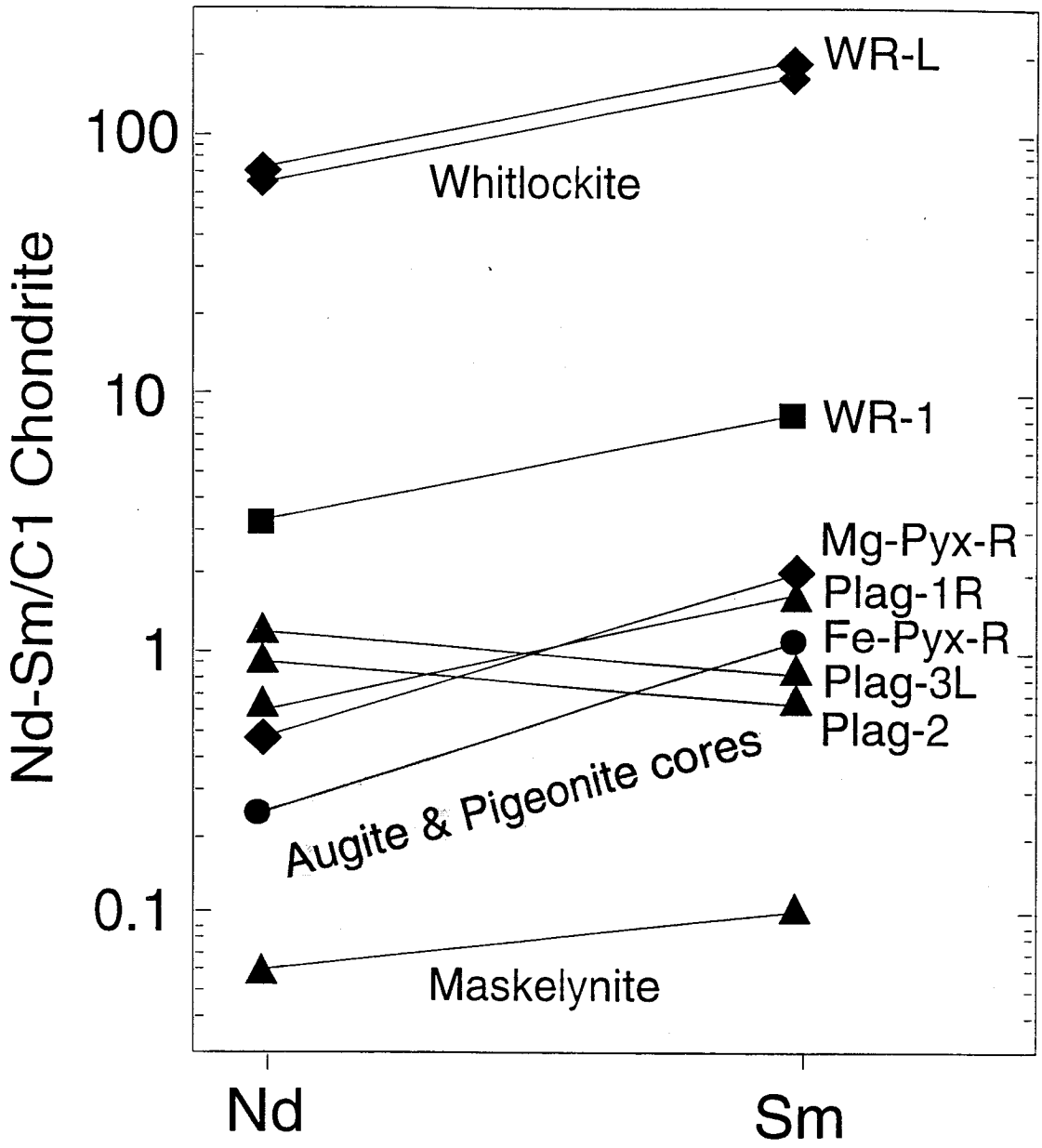
Nd-Sm/C1 Chondrite
100
10
1
0.1
Nd
Sm
WR-L
Whitlockite
WR-1
Mg-Pyx-R
Plag-1R
Fe-Pyx-R
Plag-3L
Plag-2
Augite & Pigeonite cores
Maskelynite

Figure 5.

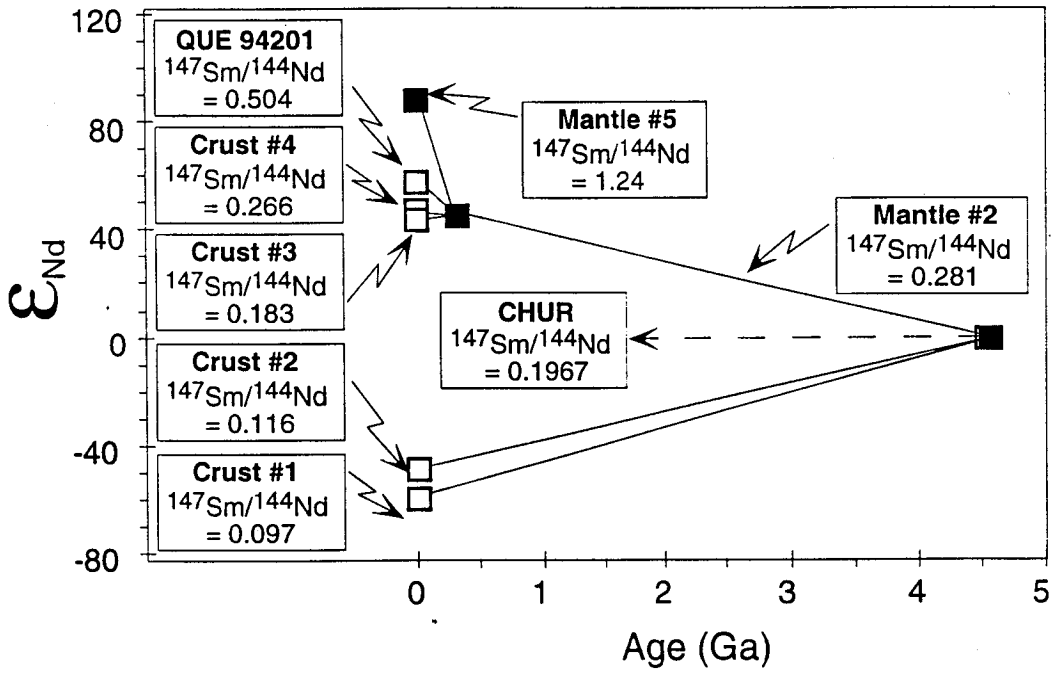
120
80
40
0
-40
-80
ε_{Nd}
QUE 94201
$^{147}Sm/^{144}Nd$ = 0.504
Crust #4
$^{147}Sm/^{144}Nd$ = 0.266
Crust #3
$^{147}Sm/^{144}Nd$ = 0.183
Crust #2
$^{147}Sm/^{144}Nd$ = 0.116
Crust #1
$^{147}Sm/^{144}Nd$ = 0.097
Mantle #5
$^{147}Sm/^{144}Nd$ = 1.24
Mantle #2
$^{147}Sm/^{144}Nd$ = 0.281
CHUR
$^{147}Sm/^{144}Nd$ = 0.1967
0
1
2
3
4
5
Age (Ga)

Figure 6.

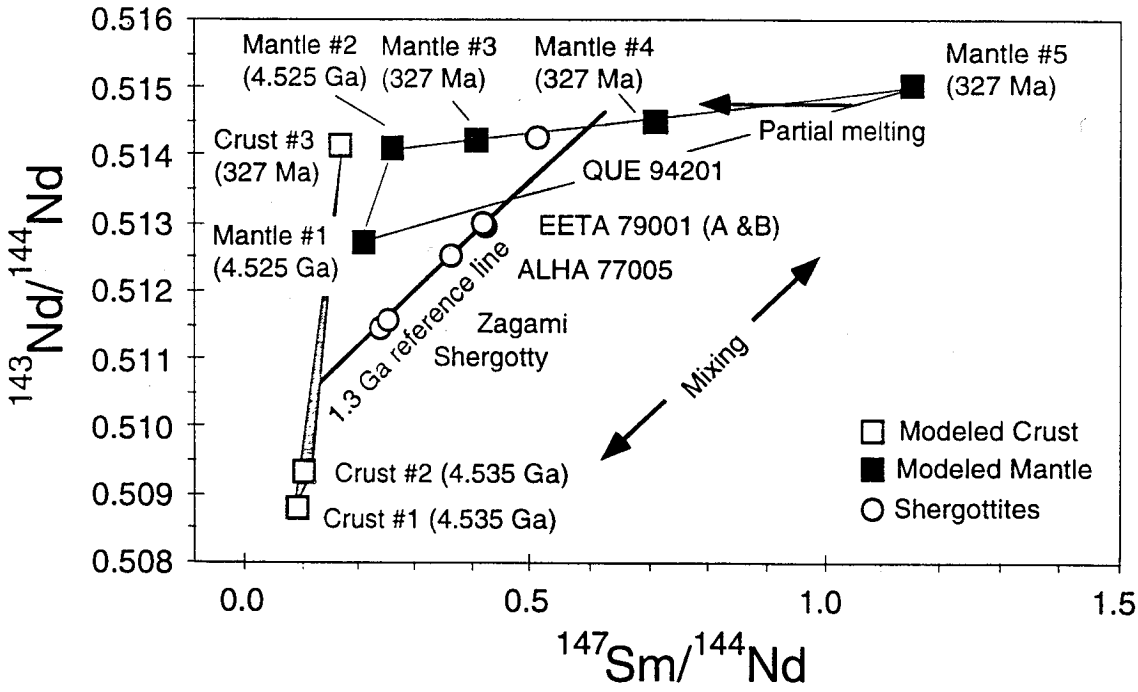
0.516
0.515
0.514
0.513
0.512
0.511
0.510
0.509
0.508
0.0
0.5
1.0
1.5
$^{143}Nd/^{144}Nd$
$^{147}Sm/^{144}Nd$
Mantle #2 (4.525 Ga)
Mantle #3 (327 Ma)
Mantle #4 (327 Ma)
Mantle #5 (327 Ma)
Crust #3 (327 Ma)
Partial melting
QUE 94201
Mantle #1 (4.525 Ga)
EETA 79001 (A &B)
ALHA 77005
Zagami
Shergotty
1.3 Ga reference line
Mixing
Crust #2 (4.535 Ga)
Crust #1 (4.535 Ga)
Modeled Crust
Modeled Mantle
Shergottites

Figure 7.

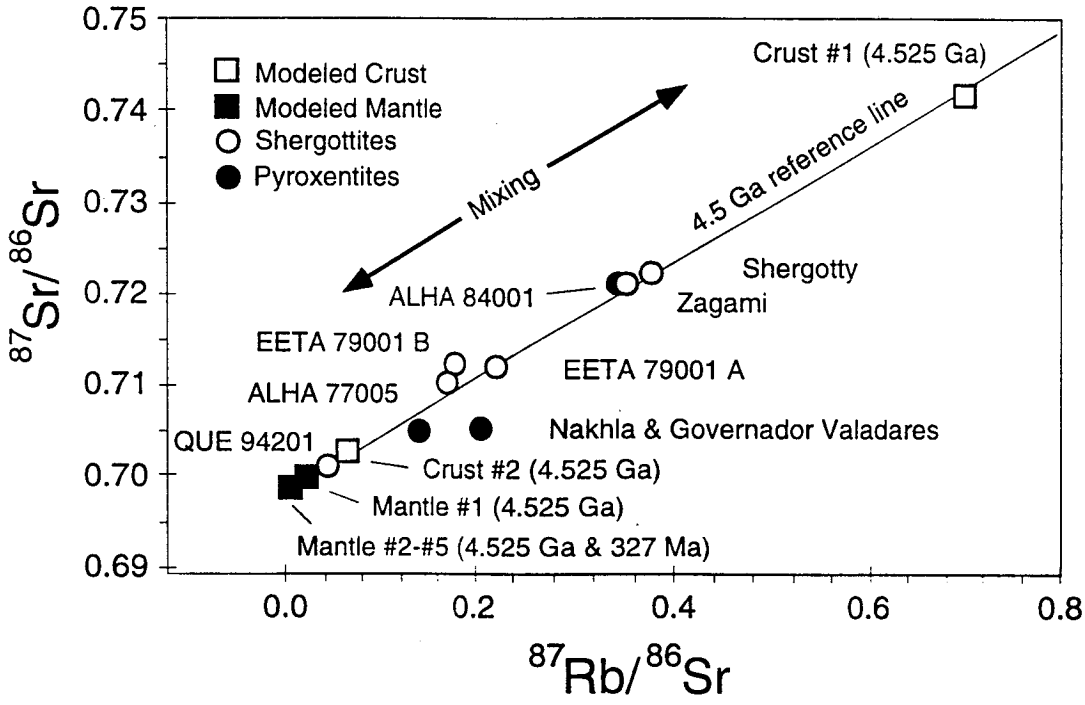
0.75
0.74
0.73
0.72
0.71
0.70
0.69
0.0
0.2
0.4
0.6
0.8
$^{87}Sr/^{86}Sr$
$^{87}Rb/^{86}Sr$
Modeled Crust
Modeled Mantle
Shergottites
Pyroxentites
Mixing
Crust #1 (4.525 Ga)
4.5 Ga reference line
Shergotty
Zagami
ALHA 84001
EETA 79001 B
EETA 79001 A
ALHA 77005
QUE 94201
Nakhla & Governador Valadares
Crust #2 (4.525 Ga)
Mantle #1 (4.525 Ga)
Mantle #2-#5 (4.525 Ga & 327 Ma)

Figure 8.